

RESEARCH

Open Access



Extracellular vesicles from mesenchymal stem cells improve neuroinflammation and neurotransmission in hippocampus and cognitive impairment in rats with mild liver damage and minimal hepatic encephalopathy

Gergana Mincheva¹, Victoria Moreno-Manzano², Vicente Felipo^{1*}  and Marta Llansola¹

Abstract

Background Patients with steatotic liver disease may show mild cognitive impairment. Rats with mild liver damage reproduce this cognitive impairment, which is mediated by neuroinflammation that alters glutamate neurotransmission in the hippocampus. Treatment with extracellular vesicles (EV) from mesenchymal stem cells (MSC) reduces neuroinflammation and improves cognitive impairment in different animal models of neurological diseases. TGF β in these EVs seems to be involved in its beneficial effects. The aim of this work was to assess if MSCs-EVs may improve cognitive impairment in rats with mild liver damage and to analyze the underlying mechanisms, assessing the effects on hippocampal neuroinflammation and neurotransmission. We also aimed to analyze the role of TGF β in the in vivo effects of MSCs-EVs.

Methods Male Wistar rats with CCl₄-induced mild liver damage were treated with EVs from unmodified MSC or with EVs derived from TGF β —silenced MSCs and its effects on cognitive function and on neuroinflammation and altered neurotransmission in the hippocampus were analysed.

Results Unmodified MSC-EVs reversed microglia activation and TNF α content, restoring membrane expression of NR2 subunit of NMDA receptor and improved object location memory. In contrast, EVs derived from TGF β —silenced MSCs did not induce these effects but reversed astrocyte activation, IL-1 β content and altered GluA2 AMPA receptor subunit membrane expression leading to improvement of learning and working memory in the radial maze.

Conclusions EVs from MSCs with TGF β silenced induce different effects on behavior, neuroinflammation and neurotransmitter receptors alterations than unmodified MSC-EVs, indicating that the modification of TGF β in the MSC-EVs has a notable effect on the consequences of the treatment. This work shows that treatment with MSC-EVs improves learning and memory in a model of mild liver damage and MHE in rats, suggesting that MSC-EVs may be a good therapeutic option to reverse cognitive impairment in patients with steatotic liver disease.

Keywords Mild liver damage, Extracellular vesicles, TGF β , Cognitive impairment, Glial activation, GABA and glutamate receptors

*Correspondence:

Vicente Felipo

vfelipo@cipfes

Full list of author information is available at the end of the article



© The Author(s) 2024. **Open Access** This article is licensed under a Creative Commons Attribution-NonCommercial-NoDerivatives 4.0 International License, which permits any non-commercial use, sharing, distribution and reproduction in any medium or format, as long as you give appropriate credit to the original author(s) and the source, provide a link to the Creative Commons licence, and indicate if you modified the licensed material. You do not have permission under this licence to share adapted material derived from this article or parts of it. The images or other third party material in this article are included in the article's Creative Commons licence, unless indicated otherwise in a credit line to the material. If material is not included in the article's Creative Commons licence and your intended use is not permitted by statutory regulation or exceeds the permitted use, you will need to obtain permission directly from the copyright holder. To view a copy of this licence, visit <http://creativecommons.org/licenses/by-nc-nd/4.0/>.

Background

Chronic liver disease induces minimal hepatic encephalopathy (MHE) with mild cognitive impairment [1, 2]. MHE is present in patients with liver cirrhosis, but mild cognitive impairment may also appear in patients with steatohepatitis, before reaching liver cirrhosis [3].

Neuroinflammation, with glial activation and increase of pro-inflammatory factors IL-1 β and TNF α , has been reported in hippocampus from patients died with steatohepatitis. This may contribute to cognitive impairment in these patients [4]. Rats with mild liver damage similar to steatohepatitis induced by carbon tetrachloride (CCl₄) injection for four weeks also show neuroinflammation in the hippocampus [5].

Neuroinflammation in the hippocampus leads to alterations in glutamatergic neurotransmission and cognitive impairment in different animal models of MHE. Reducing hippocampal neuroinflammation in hippocampus with different treatments as sulforaphane, cyclic GMP or anti-TNF α (Infliximab) reverse neurotransmission alterations and improves cognitive impairment, mainly spatial learning and memory, in rats with hyperammonemia and MHE [6–8]. Rats with mild liver damage induced by CCl₄ injection also show neuroinflammation in the hippocampus associated with altered glutamatergic and GABAergic neurotransmission and impaired spatial learning and memory [5].

Extracellular vesicles (EVs) from mesenchymal stem cells (MSC), including those derived from human adipose tissue, have beneficial effects on neurodegenerative diseases by mechanisms involving reduction of neuroinflammation [9, 10].

In rats with hyperammonemia and MHE, injection of MSC-EVs reduce neuroinflammation in the hippocampus and improves cognitive function [11]. Adipose tissue derived EVs also show beneficial effects in metabolic diseases involving multi-organ crosstalk, including chronic liver disease [12].

TGF β is a multifunctional cytokine with multiple functions in different tissues and pathological situations [13]. TGF β has a main role in the induction of hepatic fibrosis [14]. In addition, TGF β modulates immune system having mainly an anti-inflammatory function. TGF β modulate T cells inducing regulatory T cells and Th17 and inhibiting activation of proinflammatory T cells, Th1 and Th2 [13, 15, 16]. In the brain, anti-inflammatory and neuroprotective actions of TGF β were reported in models of multiple sclerosis, stroke or Alzheimer disease [17–19].

Izquierdo-Altarejos et al. [11] showed that MSC-EVs reverse neuroinflammation and alterations in neurotransmission in hippocampal slices ex vivo from rats with hyperammonemia and MHE. Moreover, they showed that the beneficial effects of MSC-EVs was mediated by

TGF β , as MSCs-EVs derived from TGF β —silenced MSCs did not reverse neuroinflammation and alterations in neurotransmission.

The aim of this work was to assess if MSC-EVs may improve cognitive impairment in rats with mild liver damage and to analyze the underlying mechanisms, assessing the effects on hippocampal neuroinflammation and neurotransmission. We also aimed to analyze the role of TGF β in the in vivo effects of MSC-EVs on hippocampal alterations and the associated cognitive impairment in rats with mild liver damage. We therefore injected rats with mild liver damage induced by CCl₄ injection with EVs from normal MSC (C-EVs) or with MSC-EVs derived from TGF β —silenced MSCs (T-EVs) and analyzed the effects on cognitive function, neuroinflammation and changes in neurotransmission in hippocampus.

Methods

The overall protocol and experimental design was prepared before the study performance but it was not registered.

Animal model and treatment with MSC-EVs

Male Wistar rats (Wistar Han IGS, Strain code 273 from Charles River, France) weighting 150–180 g were used. Rats were housed under standard conditions: 22 °C and 40–60% humidity and light–dark cycle of 12:12 h, with standard diet and food and drink at libitum.

To induce liver damage, rats were intraperitoneally injected 3 times/week during 4 weeks with 1 mL/kg body weight of CCl₄. CCl₄ was prepared 1:10 (v:v) in corn oil as described by [5, 20, 21]. Control rats were intraperitoneally injected with 1 mL/kg of corn oil.

Rats were treated with EVs from normal MSCs (C-EVs) or from TGF β knockdown MSCs (T-EVs). They were administered twice (at 2 and 3 weeks of CCl₄ treatment) as an intravenous injection at 50 μ g in 300 μ L of phosphate buffered saline (PBS). Control rats were injected with PBS (vehicle).

Rats were divided in six groups: Control rats injected with vehicle (CV); Control rats injected with C-EVs (CE); Control rats injected with T-EVs (CE-T); CCl₄ rats injected with vehicle (CC); CCl₄ rats injected with C-EVs (CCE); CCl₄ rats injected with T-EVs (CCE-T). A total of 18 rats per group were used and total number of animal used was 108. For each variable/parameter showed in results, a priori estimation of the sample size needed was calculated with the online calculator GRANMO using previous experimental data from similar studies in the research group to estimate standard deviation and size effect. Each cage containing 3 rats was randomly allocated in any of the treatment or control groups. The order of rats or samples in each experiment was always

one rat of each group sequentially. There were no animal exclusions. Data points that were considered outliers (indicated by Graphpad PRISM software used for statistical analysis) or that experimental result is missing or wrong due to technical failures were excluded. Different experimenters and investigators performed the allocation and experiments, the outcome assessment and the data analysis.

The experiments were approved by the Ethic Committee (Comité Ético de Experimentación Animal, CEEA) of Centro de Investigación Príncipe Felipe (Tratamiento con exosomas de células mesenquimales en modelos animales de encefalopatía hepática. Mecanismos implicados, no 2019–2021) and the Conselleria de Agricultura de la Generalitat Valenciana (2020/VSC/PEA/0042, approved on 03-03-2020) and they were performed in accordance with the guidelines of the Directive of the European Commission (2010/63/EU) for the care and handling of experimental animals. No adverse effects are expected in the animals included in these experiments, except for some discomfort from the CCl_4 and MSC-EVs injections. The animal model only involves mild liver damage and inflammation and mild cognitive and motor impairments. Stress was minimized by accustoming the animals to handling by the experimenters. The work has been reported in line with the ARRIVE guidelines 2.0.

MSC culture and EVs isolation

Human adipocyte-derived mesenchymal stem cells, kindly given by HistoCell Ltd. (Spain), obtained from subcutaneous fat as previously described [22] of five different female donors, were used for EVs isolation. All donors gave written informed consent, and all procedures complied with the principles of the Declaration of Helsinki and were approved by the Ethics Committee of the Basque Country Health System (CEIC-E, Spain; Protocol no. E08-30) as was indicated in [22]. MSCs were characterized by Castro et al. [22] according to International Society of Cell Therapy (ISCT) minimum criteria for adipose-derived stromal and stem cells. Immunophenotypic analyses by flow cytometry revealed positive expression (>95%) of CD13, CD44, CD73, CD90 and CD105, and negative expression (<2%) of CD14, CD19, CD34, CD45 and HLA-DR [22]. The adherent culture of MSCs exhibited the expected fibroblast-like spindle-shaped morphology. Cells also showed multipotency capacity to differentiate towards adipogenicity, chondrogenic and osteogenic lineages, as confirmed by corresponding differentiation assays [22]. For EVs isolation, MSCs were used at passage 4–6. Cells were expanded and grown in growth medium (GM: high glucose DMEM basal medium supplemented with 20% FBS (previously centrifuged at 100,000 g for 1 h and then filtered through

0.2- μm filter for EVs depletion), 100 units/mL penicillin and 100 $\mu\text{g}/\text{mL}$ streptomycin and 2 mM l-glutamine). Each culture and isolation round consisted of 15 plates (diameter: 150 mm) at a seeding density of 750,000 cells/plate. Sub-confluent cells were incubated in GM for 48 h and then media were collected and cleared from detached cells and cells fragments by centrifugation at 300 \times g and then, the supernatant at 2000 \times g for 10 min, respectively. Subsequently, apoptotic bodies and other cellular debris were pelleted by centrifugation of the resulting supernatant at 10,000 \times g for 30 min. EVs were then pelleted from the previous resulting supernatant at 100,000 \times g for 1 h. The EV pellets were washed with PBS and centrifuged at 100,000 \times g for 1 h. The EVs were finally suspended into 100 μL PBS. Protein content was measured using the Pierce BCA-200 Protein Assay Kit (ThermoFisher, Grand Island, NY, USA) according to the manufacturer's instructions and samples were stored at -80°C .

Methods for hTGF β 1-shRNA design, cloning and lentivirus production

For lentivirus production, two different target sequences to deplete human TGF β 1 (TGF β #1: 5'-GCA GCT GTA CAT TGA CTT T; TGF β #2: 5'-CAA GCA GAG TAC ACA CAG CAT) were cloned for expression as shRNA into the pLL3.7 vector (plasmid #11,795; Addgene), which encoded GFP in a separate locus. To generate this constructs, sense and antisense oligonucleotides were annealed and ligated into the HpaI/XhoI sites of the pLL3.7 vector. Control condition includes pLL3.7 empty vector. Briefly, HEK293T cells were co-transfected with the pLL3.7 constructs and the packaging plasmids. Lentiviral particles in the medium were concentrated by centrifugation at 26,000 rpm during 2 h, resuspended in chilled PBS, aliquoted and stored at -80°C . Viral titers were obtained by infecting HEK293T cells with serial dilutions of concentrated lentiviruses and sorting of GFP-positive cells by FACS 72 h after infection. For extracellular vesicles purification, HEK293T cells were infected at a multiplicity of infection (moi) of 5. The complete medium was replaced with fresh medium 16–18 h after infection. The infection efficiencies were higher than 70% in all cases, determined by the number of cells expressing GFP. The knockdown expression efficiency, evaluated by western blotting using the TGF β antibody (Abcam), was higher than 60% over the total protein expression either in 293 T cells after plasmid transfection, and in MSC after lentiviral.

Detection into hippocampus of the intravenous injected extracellular vesicles

A different group of rats ($n=2$) were intravenously injected with fluorescently labelled EVs. Both types of

EVs were labelled with the lipophilic dye Dil (Sigma, 40 µg/mL) for 15 min. Rats were intravenously injected with 50 µg of labelled EVs and were anesthetized 72 h later with sodium pentobarbital and transcardially perfused with 0.9% saline followed by 4% paraformaldehyde in 0.1 M phosphate buffer (pH 7.4). Fixed brains were extracted and frozen in OCT (Embedding Matrix for frozen sections; CellPath). Brains were cut at 7 µm sections on a cryostat and stained with Iba1 (1:300, WAKO), followed by donkey anti-rabbit Alexa 488 secondary antibody (1:400, Invitrogen) and DAPI staining. Images were acquired at 63X (oil objective, 63X Plan-Apochromat-Lambda Blue 1.4 N.A) with a Leica TCS SP8 (Leica Microsystems Heidelberg GmbH, Mannheim, Germany) inverted laser scanning confocal microscope.

Proteomics characterization of EVs from wild type MSCs and from TGFβ knockdown MSCs: analysis of differential expression

The proteomic analysis was performed in the proteomics facility of SCSIE University of Valencia. Triplicate samples of EVs in PBS (20 µg), isolated from wild type MSCs and from MSCs with silenced TGFβ were processed for proteomic analysis in the proteomics facility. Exosomes were lysed for 5 min. at 95 °C. Then 5 µg of total protein extracted were solved in 50 mM ammonium bicarbonate in solution digestion. Cysteine residues were reduced at 60 °C for 20 min. Sulfhydryl groups were alkylated with 5.5 mM iodo acetoamidyl in 50 mM ammonium bicarbonate in the dark at r.t. for 30 min. The whole alkylated samples were digested with 200 ng of trypsin o.n. at 37 °C. Digested peptide solutions were acidified to 1% TFA.

Tandem mass spectrometry (LC/MS/MS) Analysis

An approximate quantity of 200 ng of digested peptides were diluted to 20 µL with 0.1% FA and loaded in an EviTip pure tip (EvoSep) according manufacturer instructions. LC-MS/MS was performed in a Tims TOF flex mass spectrometer (Bruker). The sample loaded in the EviTip pure was eluted to an analytical column (EvoSep 15 cm×150 µm, 1.5 µm; EvoSep) by the EvoSep One system, and resolved with the 30 SPD chromatographic method defined by the manufacturer. The eluted peptides were ionized in a captive Spray with 1700 V at 200 °C, and analysed in a diaPASEF mode with the following settings: for TIMS, Mode: custom; 1/K0: 0.6–1.6 V s/cm²; ramp time: 100 ms; Duty Cycle: 100%; Ramp Rate: 9.42 Hz; Ms Averaging:1; Auto Calibration: off and for MS settings, Scan: 100-1700 m/z; Ion Polarity: Positive; Scan Mode: diaPASEF [23]. The system sensitivity was controlled with 50 ng of HELA digested proteins: 6400

proteins identified with the 30 SPD gradient in diaPASEF mode.

Protein quantification

The PASER system (Bruker) was used to send the data for Quantitation with DIAnn v1.8.2 (https://osf.io/q8kfc/?view_only=5e77d3c62563468280fd09265583dbbd). First, an in silico-predicted spectral library was built from the SwissProt human database. After, the diaPASEF raw data files were analysed. Excel documents were generated with the unique genes and protein groups quantified with FDR ≤ 1%. Due to the grouping algorithm of DIAnn quantification was performed using the unique genes group excel file. But, for some proteins that have not an associated gene name the protein groups file was used for analysis.

Differential expression (DE) analysis

DE analysis was done by Marker View 1.3. (SCIEX). Statistics for the reduction of the dimensionality were done. T-test statistical analysis were performed between wild type EV samples and samples of EVs from silenced TGFβ-MSCs. Differential genes by differential analysis were further analysed by String (<https://string-db.org/>) for functional analysis.

Analysis of liver damage markers in serum

Serum was extracted from the saphenous vein in blood collection tubes (BD Microtainer SST). Samples were sent to be analysed in Laboratorio Dr. F. Echevarne, Analisis, S.A. Liver damage markers alanine transaminase (GPT/ALT), aspartate transaminase (GOT/AST) and alkaline phosphatase (AP) were analysed.

Liver histology

At 4 weeks of CCl₄ administration rats were anaesthetized with sodium pentobarbital (1 mL/kg body weight) and trans-cardially perfused with 0.9% saline followed by 4% paraformaldehyde (PFA) in 0.1 M phosphate buffer (pH 7.4). Livers were taken out, post-fixed in PFA for 24 h at 4 °C and embedded in paraffin. Five-micrometer thick sections were obtained in a microtome and mounted on glass slides. Liver damage grade was analysed with hematoxylin and eosin (H&E) and Masson trichrome stains. Liver damage was graded using a scoring system as in Kleiner et al. [24]. The histological features considered were lobular inflammation (0–3), and fibrosis grade (0–3).

Novel object location (NOL) memory test

The test was performed in an open-field arena with visuospatial cues on the walls as in [25]. Habituation was performed during 5 days by allowing the rats freely explore

the empty arena for 5 min. On day 6 two identical objects were placed in the arena and after freely exploring for 3 min, the rat was put into its cage for two hours. After that, one of the objects was moved to a different location and allowing the rat to freely explore again for 3 min. A discrimination ratio was calculated as the difference between the time spent exploring the object whose location had been changed and the object that was still in its initial position, divided by total exploring time.

Radial maze

Radial maze was performed as in Hernández-Rabaza et al. [6] in a maze with 8 arms radially distributed from a central area. Habituation was performed during two sessions, in which rats freely explored for 5 min, with pellets along all arms in the first session and in the second session pellets were located at the end of each arm. Test was performed during 4 days (three trials per day). The task involved locating pellets placed at the end of four arms according to a random configuration, which is variable for different rats but that kept invariable for each rat throughout training. Entries to arms without pellets are considered spatial reference errors. Number of reference errors is a measure of spatial memory. Working errors are defined as entries in arms already visited in the same trial and number of working errors is a quantification of working memory. We calculated a learning index as the number of correct choices (first entries to baited arms) minus number of learning errors (first entries to unbaited arms).

Immunohistochemistry

Rats were anaesthetized with sodium pentobarbital (1 mL/kg body weight) and transcardially perfused with 0.9% saline followed by 4% paraformaldehyde in 0.1 M phosphate buffer (pH 7.4). Whole brains were removed and immersed in the same fixation solution for 24 h at 4 °C. After that, the brains were embedded in paraffin and five- μ m sections were cut on a microtome and mounted on a coated glass slide. Sections were deparaffinized for 1 h at 62 °C, rehydrated and antigen retrieved (Tris-EDTA buffer or sodium citrate buffer, depending on antibody brand recommendation). After that, sections were incubated with 3% H₂O₂ for 15 min to block endogenous peroxidases, and with 5% normal goat serum (NGS) for 1 h. Sections were incubated with primary antibodies overnight at 4 °C. Primary antibodies used were: anti-ionised calcium binding adapter molecule 1 (IBA1) (Wako 019-19741, 1:300); anti-Glial Fibrillary Acidic Protein (GFAP) (Sigma G3893, 1:400), anti-IL-1 β (Abcam ab9722, 1:300), anti-TNF α (Abcam ab6671, 1:300). Sections were washed and incubated with biotinylated secondary antibodies goat anti-rabbit and goat anti-mouse

(Vector Laboratories, 1:200) for 1 h at room temperature. After that, they were incubated with Avidin Biotin Complex (ABC) (Vector Laboratories) for 30 min and finally diaminobenzidine (DAB) was added for a maximum of 10 min. Mayer's hematoxylin (DAKO S3309; Ready to use) for 5 min was used to counterstain nuclei.

Analysis of astrocytes and microglia activation

Sections stained with IBA1 or GFAP were scanned with Aperio Versa system (Leica Biosystems) and images were taken with ImageScope software (Leica Biosystems). Analysis of IBA1 and GFAP staining was performed in the whole hippocampus (10 random fields per animal at 40X). Reduced perimeter of microglia (due to amoeboid shape) was considered as a measure of activation. The perimeter of individual IBA1+ cells was measured with ImageProPlus software. Astrocytic activation was measured as percentage of GFAP stained area with Image J software.

Analysis of IL-1 β

Analysis of IL-1 β in the hippocampus was performed on 10 40X-fields per rat randomly photographed. The mean gray value in the pyramidal neurons of the CA1 layer was calculated using ImageJ software. Besides, the intensity of IL-1 β staining in the CA1 area was measured with the image J ROI tool selecting specifically the area. The mean intensity of the background was used as a blank. The results were expressed as the mean intensity of the images per animal.

Analysis of protein content by western blot

Rats were euthanized by decapitation. Hippocampi were dissected and stored at -80°C. Hippocampi were homogenized in 50 mM TRIS-HCl pH 7.5, 50 mM NaCl, 10 mM EGTA, 5 mM EDTA and protease and phosphatase inhibitors for analysis by Western blot as in [26]. Bicinchoninic acid (BCA) method (Pierce Rockford, IL, USA) was used to quantification of total protein content in each hippocampus sample. Twenty-five μ g of protein were loaded in 10 or 15% SDS gels. Immunoblots were performed with antibodies against: TNF- α (1:500, AF-510-NA) and IL-1 β (1:250, AF-501-NA) from R&D SYSTEMS (Minneapolis, MN, USA); GAD65 (1:1000, ab26113) and GAD67 (1:1000, ab26116), from Abcam (Cambridge, UK); as loading control GAPDH (1:15000, MAB374, Millipore (Burlington, MA, USA)) or β -actin (1:5000, ab6276, Abcam) were used. Secondary antibodies (1:4000) were IgGs conjugated with alkaline phosphatase (Sigma, St. Louis, MO, USA). The images were captured using a Hewlett Packard ScanJet 5300C and band intensities were quantified using AlphaImager 2200 software.

Membrane expression of subunits of GABA, AMPA and NMDA receptors

It was analysed by cross-linking with bis(sulfosuccinimidyl) suberate (BS3) (Pierce, Rockford, IL, USA) as described by Cabrera-Pastor et al. [27]. BS3 is a cross-linker that reacts with the proteins in the external part of the cell membrane, resulting in the formation of large protein aggregates which may not enter the gel in the electrophoresis system. BS3 leaves intracellular proteins intact. Thus, when BS3-treated samples are run on an electrophoresis gel, the intracellular proteins run to their normal location according to their Mr while the membrane proteins do not penetrate the gel. For each experiment and sample, a slice treated with BS3 and another not treated with BS3 are run. In the samples non-treated with BS3 all the protein (both intracellular and membrane) runs at its normal Mr. In this way, the difference between the intensities of the bands of the samples incubated without and with BS3 is a measure of the amount of protein present in the cell membrane.

Rats were sacrificed by decapitation and the dissected hippocampi were put into ice-cold Krebs buffer (in mmol/L): NaCl 119, KCl 2.5, KH₂ PO₄ 1, NaHCO₃ 26.2, CaCl₂ 2.5, and glucose 11, aerated with 95% O₂ and 5% CO₂ at pH 7.4. 400 µm thick cross sections were cut with a chopper and added to tubes with cold Krebs buffer, with or without 2 mM BS3. Incubation with BS3 was performed for 30 min at 4 °C with gentle shaking. Cross-linking was terminated by adding 100 mM glycine (10 min, at 4 °C). The slices were homogenized in a lysis buffer (66 mM Tris-HCl (pH 7.4), 1% SDS, 1 mM EGTA, 10% glycerol, 0.2 mg/ml leupeptin, 1 mM NaF, and 1 mM sodium orthovanadate) by sonication for 20 s. Samples were analysed by Western blot using antibodies against NR1 (NMDA Receptor subunit 1) (1:1000, BD Biosciences, New Jersey, USA), NR2B (NMDA Receptor subunit 2B) (1:1000, Millipore), NR2A (NMDA Receptor subunit 2A) (1:1000; Millipore), GluA1 subunit of AMPA receptor (1:1000; Millipore) GluA2 subunit of AMPA receptor (1:2000; Millipore), GABA_A-β3 subunit (1:1000, Abcam), GABA_A-α1 subunit (1:1000, ab8341-50, Abcam) GABA_A-α2 subunit (1:1000, BS-12061R, Bioss, Woburn, MA, USA), GABA_A-α5 subunit (1:1000, GTX31004, Genetex, Irvine, CA, USA), GABA_A-γ2 subunit (1:500, ab87328, Abcam), NKCC1 (1:1000, t4-s, IOWA UNIV, USA) and KCC2 (1:1000, 07-432, Millipore). The membrane expression of proteins was calculated as the difference between the intensity of the bands (after normalization with intensity of loading control band of actin or GAPDH) without BS3 (total protein) and with BS3 (non-membrane protein) [27].

Statistical analysis

GraphPad Prism software v. 9.5.0 was used for statistical analysis. Data are expressed as mean ± SEM. Statistical analysis was carried out using one-way ANOVA and the indicated post-hoc test or two-way ANOVA with repeated measures and the indicated multiple comparisons test, when appropriate. Data that did not show normal distribution were analysed with the nonparametric Kruskal–Wallis test and Dunn's test for multiple comparisons. When standard deviations (SDs) were not equal, Welch's ANOVA followed by the indicated post-hoc test was used. A confidence level of 95% was considered as significant.

Results

EVs injected intravenously reach microglia and neurons in the hippocampus

To assess if EVs reach the hippocampus we labelled them fluorescently and assessed by immunofluorescence its presence in microglia (by double immunofluorescence with the microglia marker Iba1) and other cell types. As shown in Fig. 1A EVs co-localize with microglia and are also present in other cell types, including cells in the granular layer of the hippocampus. C-EVs and T-EVs behaved similarly, no differences were observed in the localization of C-EVs and T-EVs into the hippocampus.

Characterization of EVs

The proteomic analysis shows that the cargo of EVs derived from MSCs with silenced TGFβ is different from that of wild type EVs. Differential expression analysis of proteomics reported 14 differentially expressed proteins, 7 up-regulated and 7 down-regulated (Fig. 1B). These proteins were mainly related to cellular metabolism and to vesicles trafficking. We also analysed the content of TGFβ in the EVs by Western blot. As shown in Fig. 1C the content of the precursor form of TGFβ is reduced in MSCs after silencing of TGFβ, as well as in T-EVs compared with C-EVs, while the mature form is not affected. In EVs from MSCs with TGFβ silenced the content of the latent form of TGFβ was 60 ± 8% of the content in EVs from wild type MSCs (n = 4 different samples of EVs used for in vivo injections).

Characterization of particles in the MSC-EVs samples by nanoparticle tracking analysis showed its distribution profile, size and concentration (Supplementary Fig. 1). Transmission electronic microscopy was also used to visualize MSC-EVs (Supplementary Fig. 2). In addition, we have checked the expression of specific protein markers of EVs by western blot. Specific detected proteins were Flotilin2, CD9 and Hsp70 (Supplementary Fig. 3).

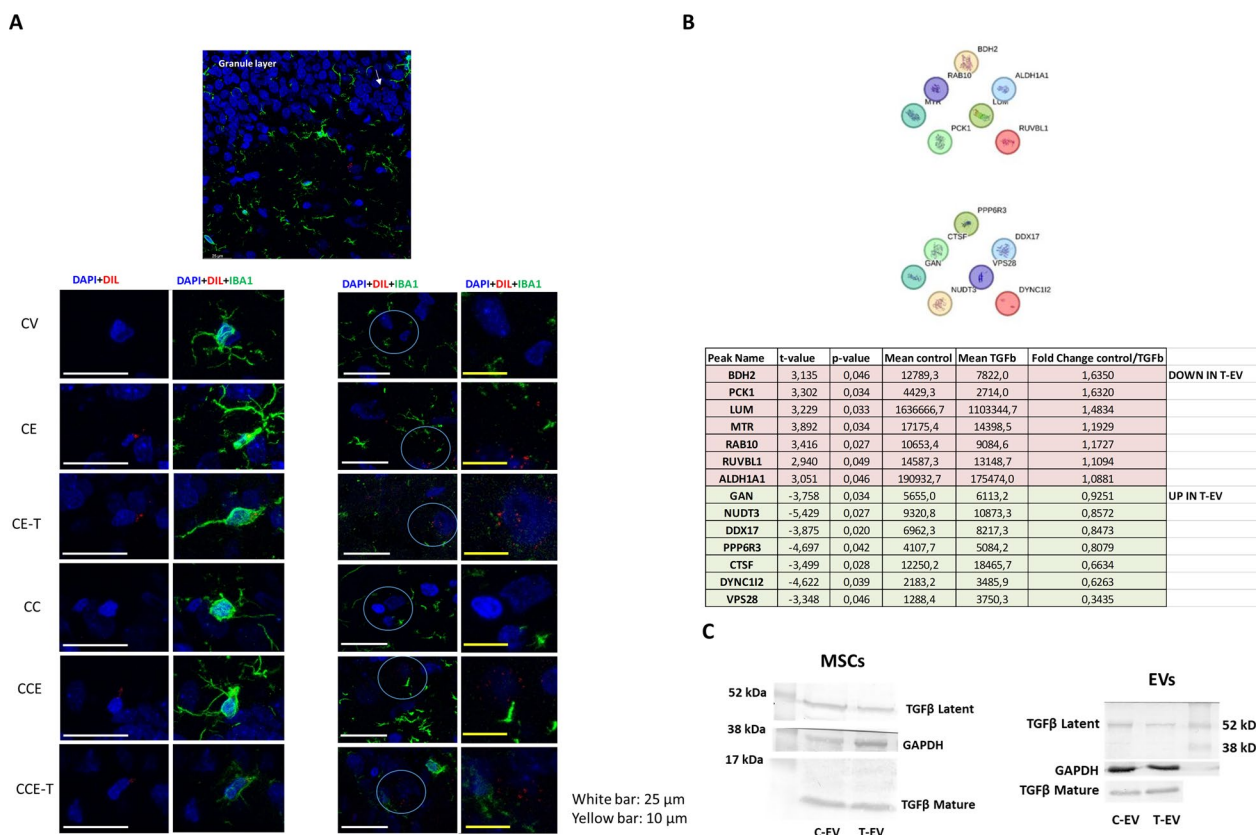


Fig. 1 EVs injected intravenously reach the hippocampus of rats. Proteomics characterization of wild type EVs and siTGFβ-EVs. **A** Fluorescent EVs (DIL, red) injected i.v. reach the hippocampus and co-localize with microglia cells stained with Iba1 (green) (left panels) and with other hippocampal cells (right panels), including cells in the granular layer (upper panel). **B** Downregulated and Upregulated proteins in siTGFβ-EVs (T-EVs) compared with control (wild type) EVs (C-EVs). **C** The content of TGFβ was analysed by Western blot in wild type MSCs and in MSCs with silenced TGFβ (left image) and in C-EVs and T-EVs (right image)

Proteomic analysis also revealed the presence of Alix (PDCD6IP), CD9 and Flotilin2 in the analysed EV samples (Supplementary Table 1).

MSC-EVs treatment does not improve liver damage as analyzed by histology or by serum hepatic enzymes in rats with mild liver damage

After 4 weeks of CCl₄ administration (CC group) rats show lobular inflammation ($p=0.0067$ compared with CV control group) (Fig. 2 A,C). Low grade of liver fibrosis can be also observed ($p=0.025$ compared with controls) (Fig. 2B, D). Lobular inflammation and fibrosis were not significantly affected by control MSC-EVs (C-EVs) in control rats (CE group) or CCl₄ rats (CCE group) or by TGFβ⁻MSC-EVs (T-EVs) in control (CE-T group) or CCl₄ rats (CCE-T group) (Fig. 2A–D).

As reported previously [21], rats with mild liver damage show increased serum levels of GPT/ALT ($p=0.042$) and of alkaline phosphatase ($p=0.0039$) after 4 weeks of CCl₄ administration. No significant increase in GOT/AST was observed in serum of these rats (Fig. 2E–G).

Treatment with C-EVs does not reduce ALT activity in serum of CCl₄ rats but increased GOT/AST ($p=0.035$) and alkaline phosphatase activity ($p=0.016$). Treatment with T-EVs did not affect any enzymatic serum marker of liver damage (Fig. 2E–G).

Effects of mesenchymal stem cells derived extracellular vesicles on spatial memory and learning in rats with mild liver damage

Spatial learning was analysed in the radial maze in 6–9 rats per group. The statistical analysis of learning index by two-way ANOVA showed a significant effect of time ($p<0.0001$; $F(3, 126)=18,16$) indicating learning of the task along trials and days. The difference between groups was also significant ($p=0.031$; $F(5, 48)=2,709$). Also, significant interaction between both factors, time and groups, was found ($p=0.0035$; $F(15, 126)=2,452$) (Fig. 3A). This analysis was followed by Uncorrected Fisher’s LSD test. All groups showed significant decreased learning index than control group at day four, except rats with mild liver damage treated with T-EVs, which were

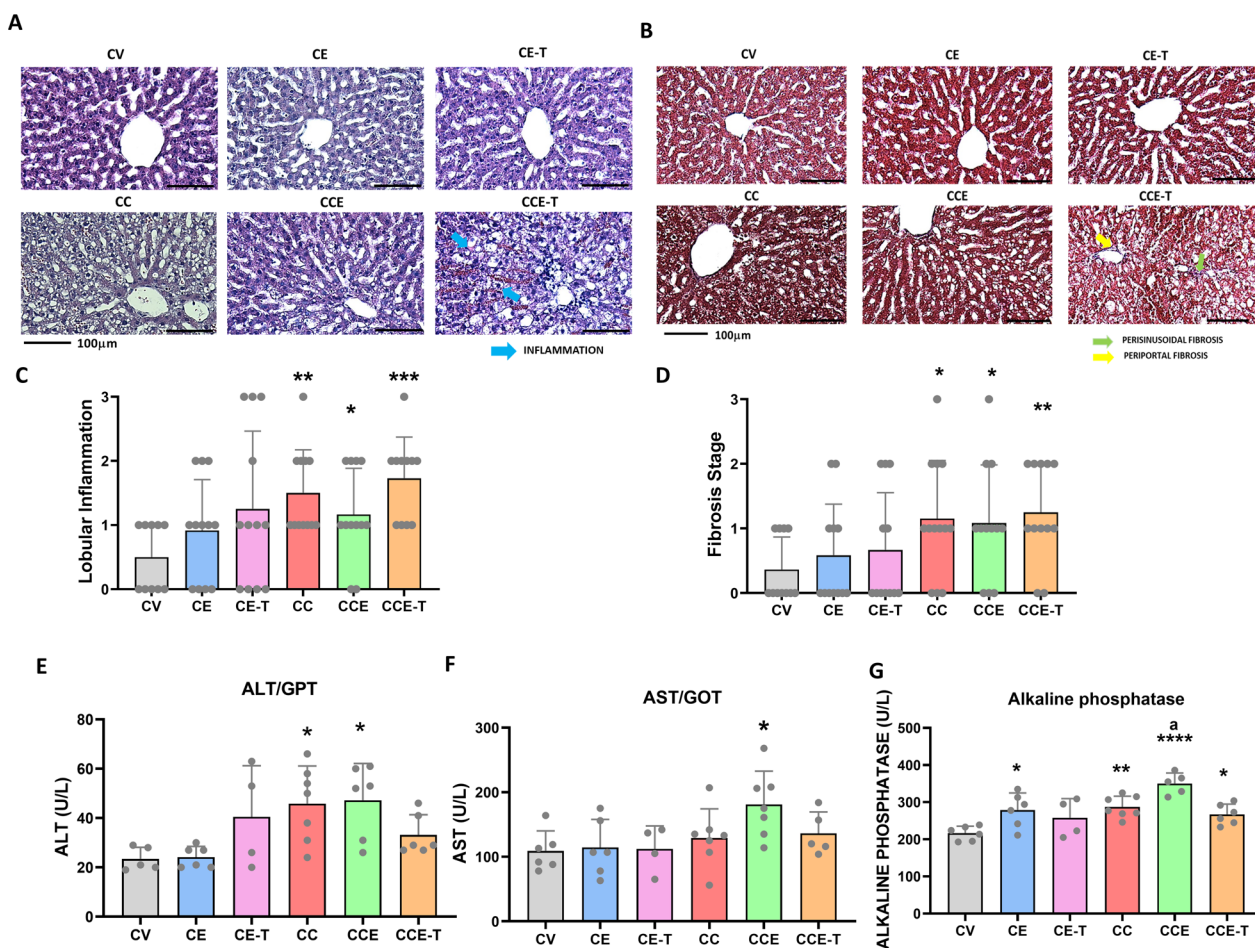


Fig. 2 MSC-EVs do not improve histological and serum markers of liver damage in rats with mild liver damage. Lobular inflammation was evaluated in H&E stained liver sections (A) and mean \pm SD of the score from 10 to 12 rats per group is shown in C. Masson staining was used to histologically evaluate liver fibrosis in other sections of the same rats (B). Fibrosis score is shown in D (mean \pm SD of 11–13 rats per group). In C, data were also analysed with Kruskal–Wallis test with $KW=9.958$, $p=0.019$ for C-EVs and KW statistic = 12.28, $p=0.0065$ for T-EVs and uncorrected Dunn’s test was used for multiple comparisons. Fibrosis data were analysed with Kruskal–Wallis test followed by uncorrected Dunn’s test. For C-EVs data were KW statistic = 7.559, $p=0.056$ and for T-EVs data were $KW=8.936$, $p=0.030$ (D). Quantification of hepatic enzymes, ALT (E), AST (F) and alkaline phosphatase (G) in serum, was performed in 4–7 rats per group. Data were analysed with One-Way ANOVA followed by Tukey’s multiple comparisons test: in E C-EVs $F(3, 20)=7550$, $p=0.0014$ and T-EVs $F(3, 18)=3,083$, $p=0.054$; in F, C-EVs $F(3, 22)=3,745$, $p=0.026$ and T-EVs $F(3, 18)=0,6609$, $p=0.59$; in G C-EVs $F(3, 20)=15,84$, $p<0.0001$ and T-EVs (Welch’s ANOVA test) $W=9,303(3000, 8746)$, $p=0.0044$. Values significantly different from control rats are indicated by asterisks: * $p<0.05$, ** $p<0.01$, *** $p<0.001$, **** $p<0.0001$ and values significantly different from CCl₄ rats are indicated by a, $p<0.05$

significantly different from CCl₄ rats without treatment, both at day three ($2,8 \pm 0.7$, $p=0.045$ in group CCE-T, compared with 1.5 ± 0.2 in CC group) and at day four (2.0 ± 0.2 in CC and 4.1 ± 0.9 for group CCE-T, $p=0.0066$). Data of learning index at day four were also analysed separately for C-EVs or T-EVs treatment: for C-EVs, Brown-Forsythe ANOVA test, $F(3,000, 9,049)=7,134$, $p=0.0093$, was followed by unpaired t with Welch correction; for T-EVs, One-Way ANOVA, $F(3, 25)=2,438$, $p=0.088$, was followed by the Uncorrected Fisher’s LSD test. At day 4, rats with mild liver damage show a reduced

learning index (CC 1.9 ± 0.27 ; $p=0.035$) compared to control rats (CV 4.2 ± 0.86). C-EVs did not improve learning index in rats with mild liver damage (CCE 1.6 ± 0.15 ; $p=0.019$ vs CV,) but even worsen learning index at day 4 in control rats (CE 1.8 ± 0.14 , $p=0.026$ compared with controls). However, treatment with T-EVs (CCE-T 4.1 ± 0.94 , $p=0.047$) improve learning index in rats with mild liver damage at day 4 (Fig. 3B).

CCl₄ treated rats also show impaired working memory. Analysis by one-Way ANOVA ($F(5, 40)=3,957$, $p=0.0052$) followed by the Uncorrected Fisher’s LSD test

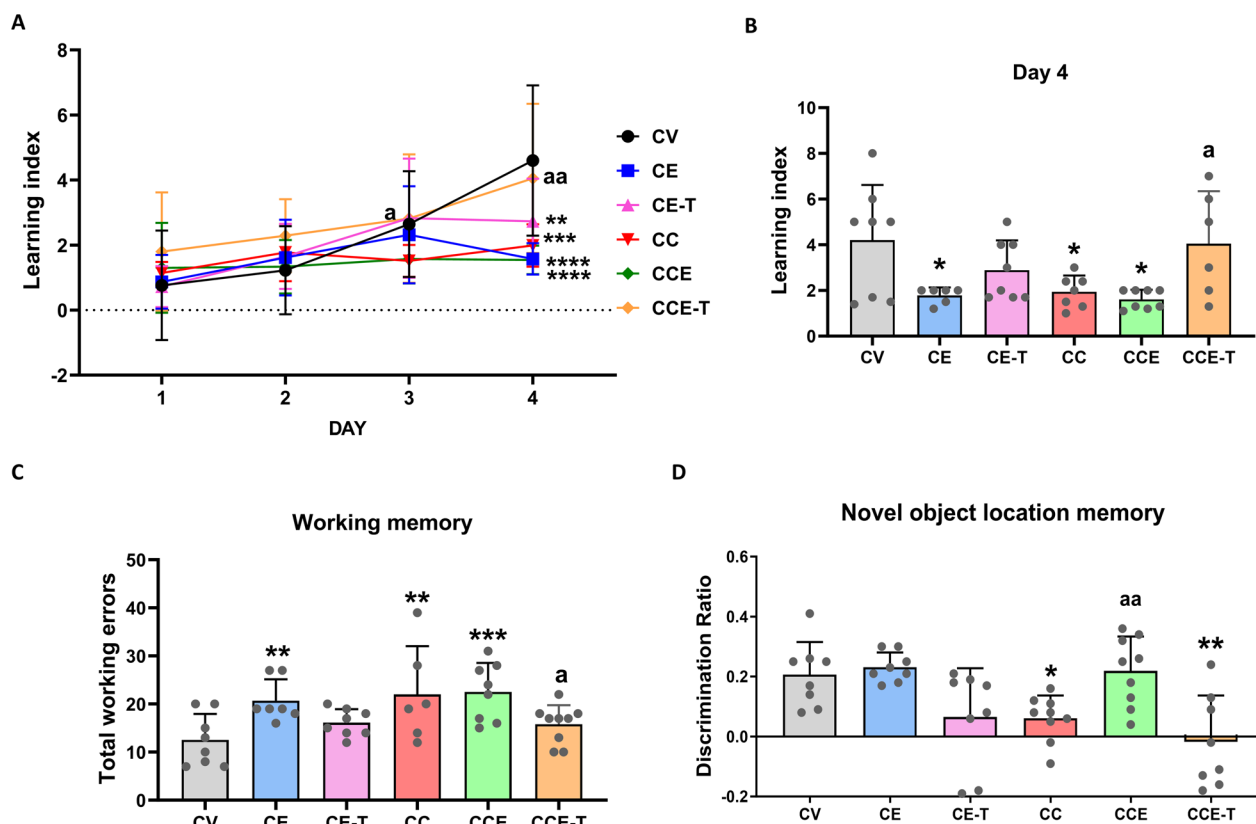


Fig. 3 Effects of MSC-EVs on spatial memory, spatial learning and working memory. Learning index (**A, B**) and Total working errors (**C**) were analysed in the radial maze at 8 weeks of CCl₄ treatment. Values are expressed as mean ± SD of 6–9 rats per group. **A** Learning index was analysed with a two-way ANOVA: time, $p < 0.0001$, $F(3, 126) = 18.16$; group, $p = 0.031$, $F(5, 48) = 2.709$ and interaction, $p = 0.0035$, $F(15, 126) = 2.452$. Post hoc analysis was performed with Uncorrected Fisher’s LSD test. **B** Analysis was performed separately for C-EVs or T-EVs treatment. For C-EVs Brown-Forsythe ANOVA followed by unpaired t with Welch correction was used: $F(3, 000, 9,049) = 7134$, $p = 0.0093$; for T-EVs One-way ANOVA was used: $F(3, 25) = 2.438$, $p = 0.088$ followed by the Uncorrected Fisher’s LSD test (**C**) One-Way ANOVA was used ($F(5, 40) = 3.957$, $p = 0.0052$) followed by the Uncorrected Fisher’s LSD test. Spatial memory in the NOL (**D**, $n = 8–9$) was assessed the third week of CCl₄ treatment. Values are expressed as mean ± SD. Data were analysed with One-Way ANOVA followed by Tukey’s multiple comparisons test (C-EVs $F(83, 30) = 6.633$, $p = 0.0014$; T-EVs $F(3, 29) = 4.172$, $p = 0.014$). Asterisks indicate significant difference compared with the control group (CV) * $p < 0.05$, ** $p < 0.01$; *** $p < 0.001$, **** $p < 0.0001$ and “a” compared with CC group a $p < 0.05$, aa $p < 0.01$

showed an increased number of total working errors during the four days in the radial maze in CC group (22 ± 4 vs 13 ± 2 errors in CV group, $p = 0.0032$). Treatment with C-EVs does not improve working memory in CCl₄ rats (23 ± 2 errors, $p = 0.001$) and increases total working errors in control rats (CE 21 ± 1.7 errors, $p = 0.0073$). In contrast, T-EVs improve working memory in CCl₄ rats, reducing working errors to 16 ± 1 ($p = 0.042$, compared with CC group) (Fig. 3C).

Spatial memory in the NOL was assessed in 8–9 rats per group the third week of CCl₄ treatment. Data were analysed with One-Way ANOVA followed by Tukey’s multiple comparisons test (C-EVs $F(3, 30) = 6.633$, $p = 0.0014$; T-EVs $F(3, 29) = 4.172$, $p = 0.014$). Rats with mild liver damage show impaired object location memory. Discrimination ratio for CC was 0.06 ± 0.025 compared to 0.21 ± 0.039 for CV, $p = 0.014$. Treatment

with C-EVs in rats with mild liver damage reverses the impairment in the novel object location test (0.22 ± 0.038 , $p = 0.0051$, compared with CC group). In contrast, T-EVs did not improve object location memory (-0.018 ± 0.055 , $p = 0.0085$ compared with CV group) (Fig. 3D).

These results indicate that normal C-EV improve object location memory in CCl₄ rats but not spatial learning and working memory while EVs lacking TFGβ improve working memory and learning index in the radial maze but not object location memory.

MSC-EVs restore membrane expression of GluN2B receptor subunit, while TFGβ⁻MSC-EVs restore membrane expression of GluA2 receptor subunit in hippocampus of rats with mild liver damage

Rats treated with CCl₄ show reduced membrane expression in hippocampus of the NMDA receptor subunits. For

NR1 subunit data were analysed with Welch’s ANOVA (C-EVs $W(3,000,18.73)=7.213, p=0.0021$; T-EVs $W(3,000, 15,90)=5,612, p=0.0081$) followed by the Dunnett’s T3 multiple comparisons test, which indicated reduction of NR1 membrane expression in CC group to $36 \pm 6\%$ of control rats ($p=0.011$), to $45 \pm 9\%$ of controls in CCE group ($p=0.041$) and to $43 \pm 12\%$ of controls in the CCE-T group ($p=0.046$) (Fig. 4A). Treatment with any type of EV do not restores membrane expression of NR1 in rats with mild liver damage. Membrane expression of NR2A was also reduced. Data were analysed by One-way ANOVA for C-EVs ($F(3, 36)=6,762, p=0.001$) followed by Fisher’s LSD test and for T-EVs with Welch’s ANOVA ($W(3,000, 16,97)=3,583, p=0.036$) followed by Unpaired t with Welch’s correction test.

NR2A membrane expression was reduced to $68 \pm 12\%$ of control rats ($p=0.022$) in CC group, to $54 \pm 10\%$ of controls ($p=0.016$) in CCE group and to $62 \pm 12\%$ of control ($p=0.023$) in CCE-T group (Fig. 4B), indicating that EVs treatment not affect membrane expression of NR2A. Membrane expression of the NR2B subunit is also decreased in the CCl_4 group without treatment or treated with T-EVs and also in the control group treated with T-EVs. Data were analysed with One-way ANOVA (C-EVs $F(3, 34)=2,360, p=0.089$; T-EVs $F(3, 29)=4,952, p=0.0068$) followed by Fisher’s LSD test: membrane expression was reduced to $62 \pm 13\%$ of control group in the CC group ($p=0.014$) and to $44 \pm 7\%$ of controls ($p=0.0014$) in the CCE-T group. Treatment with T-EVs decreased membrane expression of NR2B in control rats

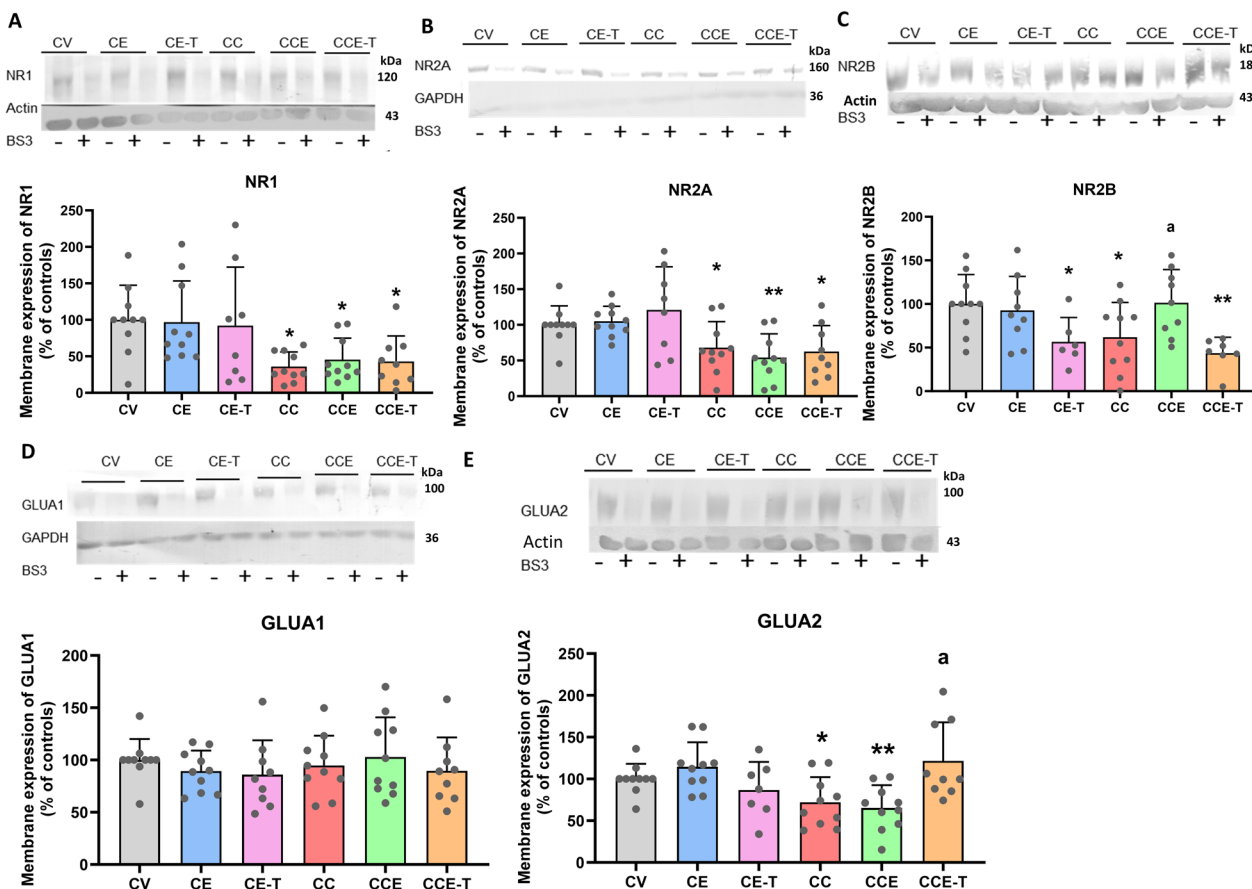


Fig. 4 Effects of MSC-EVs on membrane expression of NMDA and AMPA receptors subunits. Membrane expression in hippocampus of NMDA receptor subunits NR1 (A), NR2A (B) and NR2B (C), and of the AMPA receptor subunits GluA1 (D) and GluA2 (E). Data are expressed as mean \pm SD. A Data were analysed with Welch’s ANOVA followed by the Dunnett’s T3 multiple comparisons test: C-EVs $W(3,000,18.73)=7.213, p=0.0021$; T-EVs $W(3,000, 15,90)=5,612, p=0.0081$. B One-way ANOVA was followed by Fisher’s LSD test for C-EVs ($F(3, 36)=6,762, p=0.001$) and for T-EVs Welch’s ANOVA followed by Unpaired t with Welch’s correction test was used ($W(3,000, 16,97)=3,583, p=0.036$). C One-way ANOVA was followed by Fisher’s LSD test: C-EVs $F(3, 34)=2.360, p=0.089$; T-EVs $F(3, 29)=4,952, p=0.0068$. D One-way ANOVA was followed by Fisher’s LSD test: ($F(5, 52)=0,4979$). E One-way ANOVA was followed by Fisher’s LSD test for C-EVs: $F(3, 36)=7,607, p=0.0005$ and by Tuckey’s post hoc test for T-EVs: $F(3, 32)=3769, p=0.020$. Asterisks indicate a significant difference in the multiple comparison tests compared with CV group * $p < 0.05$, ** $p < 0.01$, and “a” compared with CC group; a, $p < 0.05$. Full-length blots are presented in the Supplementary Figs. 2A–F

to $57 \pm 11\%$ of control group, ($p=0.015$). But treatment with C-EVs normalized membrane expression of NR2B in rats with mild liver damage ($101 \pm 13\%$ of control group, $p=0.029$ compared with CC group) (Fig. 4C).

Regarding AMPA receptor subunits, membrane expression of GluA1 subunit was not altered in rats treated with CCl_4 nor by EVs. Data were analysed with One-way ANOVA ($F(5, 52)=0.4979$) (Fig. 4D). Membrane expression of the GluA2 subunit was analysed by One-way ANOVA (C-EVs: $F(3, 36)=7,607$, $p=0.0005$ and T-EVs: $F(3, 32)=3,769$, $p=0.020$) followed by Fisher's LSD test for C-EVs and by Tuckey's test for T-EVs. Rats with mild liver damage show reduced membrane expression of GluA2 subunit compared to control rats ($72 \pm 9\%$, $p=0.024$). Treatment with T-EVs reversed this alteration ($122 \pm 15\%$ of control rats, $p=0.013$) while C-EVs did not ($65 \pm 9\%$, $p=0.0061$ compared with control group) (Fig. 4E).

Effects of MSC-EVs and TFG β -MSC-EVs on membrane expression of GABAA receptor subunits in the hippocampus

GABA_A receptors and GABAergic neurotransmission also modulate hippocampal-dependent memory [5, 28–32]. We therefore also analyzed several parameters modulating GABAergic neurotransmission in hippocampus.

We analyzed by western blot the content of the glutamic acid decarboxylase isoforms GAD65 and GAD67, responsible for GABA synthesis, in 8–10 rats per group. Data of GAD65 were analysed with One-Way ANOVA (C-EVs $F(3, 34)=2,947$, $p=0.047$; T-EVs $F(3, 32)=3,073$, $p=0.042$) followed by the Uncorrected Fisher's LSD test. The content of GAD65 ($65 \pm 7\%$, of controls, $p=0.015$) was reduced in hippocampus of rats with mild liver damage and was increased to normal levels by treatment by treatment with both types of EVs ($105 \pm 10\%$ of controls with C-EVs ($p=0.011$ compared with CC group) and $103 \pm 9\%$ with T-EVs, $p=0.011$) (Fig. 5A). Data of GAD67 were analysed with One-Way ANOVA (C-EVs $F(3, 36)=5,218$, $p=0.004$; T-EVs $F(3, 36)=5,756$, $p=0.0025$) followed by the Tukey's multiple comparisons test. The content of GAD67 was also reduced in hippocampus of rats with mild liver damage ($69 \pm 7\%$ of controls, $p=0.018$) and was not affected by treatment with any type of EVs in these rats ($68 \pm 5\%$ of controls, $p=0.02$ for CCE group and $67 \pm 2\%$ of controls, $p=0.011$ in CCE-T group) (Fig. 5B). These data suggest decreased GABA synthesis that may affect GABAergic neurotransmission.

We also analyzed the effects on membrane expression of the $\alpha 1$, $\alpha 2$, $\alpha 5$, $\beta 3$ and $\gamma 2$ subunits of GABA_A receptors and of the chloride transporters KCC2 and NKCC1, in 5–10 rats per group. For membrane expression of the $\alpha 1$ subunit data were analysed with One-way

ANOVA (C-EVs $F(3, 36)=4,505$, $p=0.0088$ and T-EVs $F(3, 36)=4,923$, $p=0.0057$) followed by the Tuckey's test, which indicated a statistically significant reduction of membrane expression of the $\alpha 1$ subunit in CCl_4 rats treated with both types of EVs ($65 \pm 7\%$ of controls in C-EV group, $p=0.015$ and $64 \pm 8\%$ in T-EV group, $p=0.019$), whereas rats with mild liver damage without EVs treatment did not show change in membrane expression of the $\alpha 1$ subunit ($93 \pm 11\%$ of controls, $p=0.92$). T-EVs also reduce membrane expression of the $\alpha 1$ subunit in control rats ($67 \pm 8\%$ of controls, $p=0.033$) (Fig. 5C). Membrane expression of the $\alpha 2$ subunit was analysed by One-Way ANOVA (C-EVs $F(3, 29)=3,265$, $p=0.035$) followed by the Uncorrected Fisher's LSD test and Welch's ANOVA (T-EVs $W(3,000, 11,47)=1,938$, $p=0.18$) followed by unpaired t test with Welch's correction. Membrane expression of this subunit was significantly increased in rats with mild liver damage ($154 \pm 21\%$ of controls, $p=0.05$) and in these rats treated with C-EVs ($165 \pm 27\%$ of controls, $p=0.02$), whereas treatment with T-EVs reversed this increase to $96 \pm 10\%$ of controls ($p=0.042$) (Fig. 5D). One-Way ANOVA was followed by the Uncorrected Fisher's LSD test for the analysis of membrane expression of $\alpha 5$ subunit in C-EVs ($F(3, 36)=3,271$, $p=0.032$) and Welch's ANOVA followed by unpaired t test with Welch's correction was used for T-EVs ($W(3,000, 19,32)=3,421$, $p=0.038$). The content in cell membrane of the $\alpha 5$ subunit was significantly reduced in rats with CCl_4 administration ($62 \pm 9\%$ of controls, $p=0.019$) and this change was reversed by EVs treatment to $100 \pm 11\%$ of controls, $p=0.018$ compared with CC group, in rats treated with C-EVs and to 118 ± 21 , $p=0.031$, in rats treated with T-EVs (Fig. 5E). Membrane expression of the $\gamma 2$ subunit was analysed by Welch ANOVA followed by the Dunnett's T3 test: $W(3,000, 16,41)=10,79$, $p=0.0004$ for C-EVs and $W(3,000, 15,26)=10,96$, $p=0.0004$ for T-EVs. Membrane expression of this subunit was significantly increased in rats with mild liver damage without treatment to $169 \pm 20\%$ of controls ($p=0.042$). Treatment of CCl_4 rats with C-EVs reverses the changes in the $\gamma 2$ subunit ($61 \pm 7\%$ of controls, $p=0.0021$ compared with CC group), and the same effect had treatment with T-EVs ($50 \pm 12\%$, $p=0.0009$ compared with CC group). In addition, membrane expression of $\gamma 2$ subunit was also significantly reduced compared with controls in CCl_4 rats treated with any type of EVs ($p=0.0027$ and $p=0.019$, respectively for C-EVs treatment and T-EVs treatment) and in control rats treated with T-EVs ($60 \pm 12\%$ of controls, $p=0.064$) (Fig. 5F). One-way ANOVA analysis of membrane expression of the $\beta 3$ subunit showed significant effects of C-EVs treatment ($F(3, 22)=21,47$, $p<0.0001$) and of T-EVs treatment ($F(3, 21)=9,299$, $p=0.0004$). Post

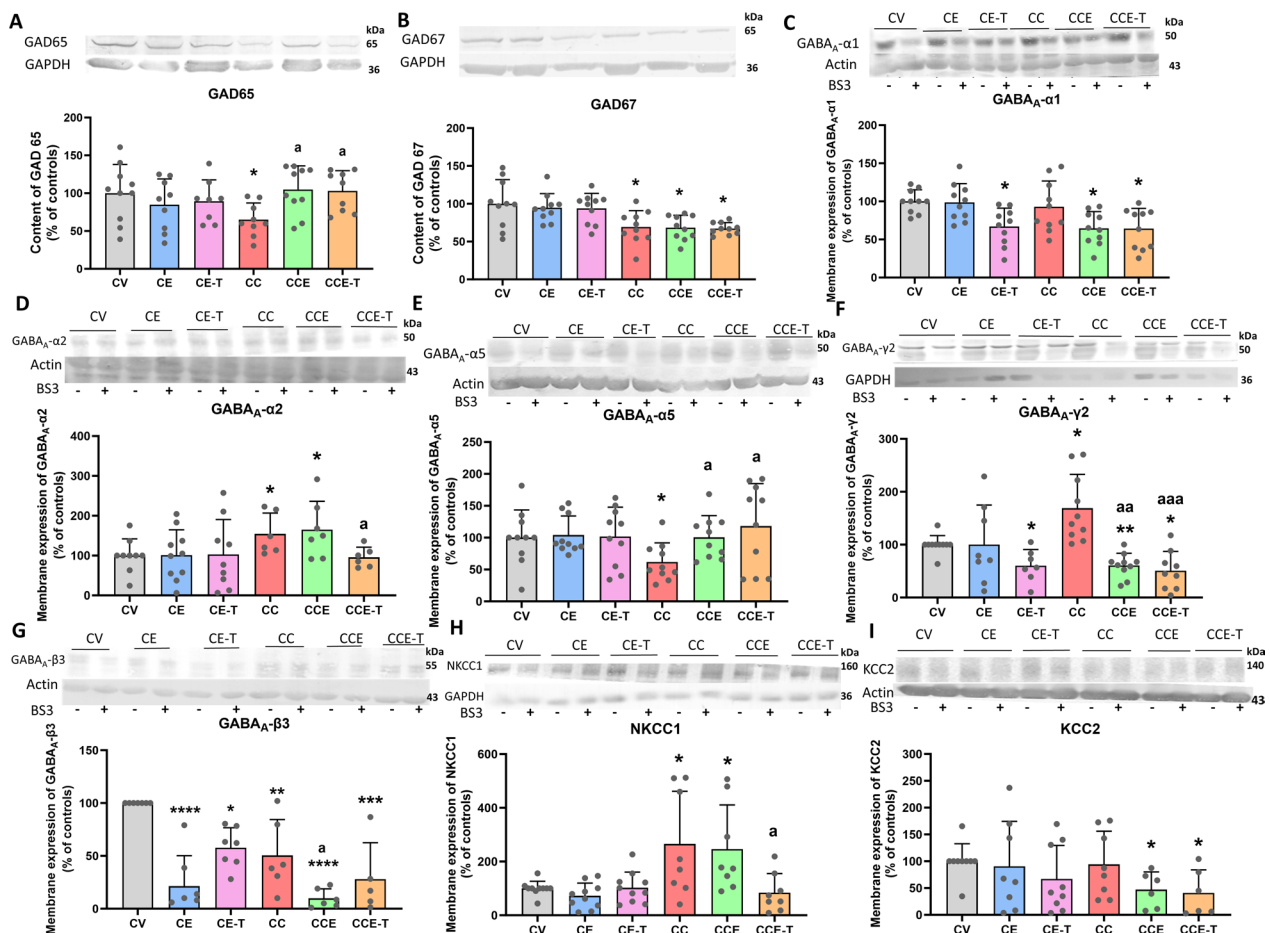


Fig. 5 Effects of MSC-EVs on some key parameters of GABAergic neurotransmission in the hippocampus. GAD65 (A) and GAD67 (B) content was analysed by Western blot. Data are expressed as mean \pm SD of 8–10 rats per group. A Data were analysed with One-Way ANOVA (C-EVs F (3, 34) = 2,947, p = 0.047; T-EVs F (3, 32) = 3,073, p = 0.042) followed by the Uncorrected Fisher’s LSD test. B Data were analysed with One-Way ANOVA (C-EVs F (3, 36) = 5.218, p = 0.004; T-EVs F (3, 36) = 5.756, p = 0.0025) followed by the Tukey’s multiple comparisons test. Data of content in the cell membrane of the GABA_A receptor subunits GABA_A-α1 (C), GABA_A-α2 (D), GABA_A-α5 (E), GABA_A-β3 (F) and GABA_A-γ2 (G), and of the chloride transporters KCC2 (H) and NKCC1 (I) are represented as mean \pm SD of 5–10 rats. C Data were analysed with One-way ANOVA followed by the Tukey’s test: C-EVs F (3, 36) = 4.505, p = 0.0088 and T-EVs F (3, 36) = 4.923, p = 0.0057. D One-Way ANOVA was followed by the Uncorrected Fisher’s LSD test (C-EVs F (3, 29) = 3265, p = 0.035) and Welch’s ANOVA followed by unpaired t test with Welch’s correction (T-EVs W (3,000, 11,47) = 1.938, p = 0.18). E One-Way ANOVA was followed by the Uncorrected Fisher’s LSD test (C-EVs F (3, 36) = 3271, p = 0.032) and Welch’s ANOVA followed by unpaired t test with Welch’s correction (T-EVs W (3,000, 19,32) = 3,421, p = 0.038). F Welch ANOVA followed by the Dunnett’s T3 test: C-EVs W (3,000, 16,41) = 10,79, p = 0.0004, T-EVs W (3,000, 15,26) = 10,96, p = 0.0004. G One-way ANOVA followed by the Tukey’s test: C-EVs F (3, 22) = 20,47, p < 0.0001 and T-EVs F (3, 21) = 9,299, p = 0.0004. H Data were analysed with Welch ANOVA (C-EVs W (3,000, 14,09) = 4,682, p = 0.018 and T-EVs W (3000, 15,56) = 1,879, p = 0.18) followed by the Unpaired t with Welch’s correction. I Data were analysed with Welch’s ANOVA (C-EVs W (3000, 13,90) = 2979, p = 0.068 and T-EVs W (3000, 14,06) = 2.750, p = 0.082) followed by the Unpaired t test with Welch correction. Asterisks indicate a significant difference in the multiple comparison tests compared with CV group * p < 0.05, ** p < 0.01, *** p < 0.001, **** p < 0.0001 and “a” compared with CC group a p < 0.05, aa p < 0.01, aaa p < 0.001. Full-length blots are presented in the Supplementary Figs. 3A, –I

hoc analysis with Tuckey’s test showed strong decrease of membrane expression of this subunit in CCl₄ rats (50 \pm 14% of controls, p = 0.0035), which was similar in control or CCl₄ rats treated with T-EVs (58 \pm 7%, p = 0.02 in controls (CE-T) and 28 \pm 15%, p = 0.003, in the CCE-T group). In CCl₄ rats treated with C-EVs, this effect was even enhanced, leading to a reduction to 10 \pm 4% of controls (p < 0.0001, compared with controls and p = 0.024

compared with CC group). In control rats treated with C-EVs reduction of membrane expression of this subunit was also strong, to 21 \pm 11% of controls (p < 0.0001) (Fig. 5G).

We also analyzed the effects on membrane expression of the chloride cotransporters NKCC1 and KCC2. In the case of NKCC1 data were analysed with Welch ANOVA (C-EVs W (3,000, 14,09) = 4,682, p = 0.018 and T-EVs W

(3,000, 15,56)=1,879, $p=0.18$) followed by the Unpaired *t* with Welch's correction. Mild liver damage increased membrane expression of NKCC1 ($266 \pm 69\%$ of controls, $p=0.049$), which was reversed by T-EVs ($86 \pm 30\%$ of controls, $p=0.040$ compared with the CC group) but not by C-EVs ($246 \pm 58\%$ of controls, $p=0.04$) (Fig. 5H). For membrane expression of KCC2 data were analysed with Welch's ANOVA (C-EVs $W(3,000, 13,90)=2,979$, $p=0.068$ and T-EVs $W(3,000, 14,06)=2,750$, $p=0.082$) followed by Unpaired *t* with Welch correction test. Membrane expression of KCC2 was not altered in CCl_4 rats but it was reduced in these rats (but not in controls) by both types of EVs (to $47 \pm 13\%$ of controls, $p=0.011$ by C-EVs and to $41 \pm 18\%$, $p=0.019$ by T-EVs) (Fig. 5I).

MSC-EVs reverse microglial activation, whereas TFGβ⁻MSC-EVs reverse astrocytes activation in hippocampus of rats with mild liver damage

Changes in GABAergic neurotransmission may be a consequence of neuroinflammation and glial activation [30]. We therefore analyzed activation of microglia and astrocytes and on the hippocampal content of IL-1β and TNFα.

Microglia activation was quantified by measurement of the reduction of cell perimeter due to acquisition of an amoeboid form. Mean of cell perimeter of the cells in several random chosen fields in the hippocampus was calculated in 4–6 rats per group. Data were analysed by Kruskal–Wallis test (Statistic=7,496, $p=0.058$) for C-EVs and by One-way ANOVA for T-EVs ($F(3, 16)=3,853$, $p=0.030$). Uncorrected Dunn's test indicated that rats with mild liver damage show activation of microglia in hippocampus, with a reduced perimeter ($273 \pm 31 \mu\text{m}$, $p=0.030$) compared to control rats ($446 \pm 62 \mu\text{m}$). Treatment with C-EVs reverse activation of microglia, returning the perimeter to $458 \pm 52 \mu\text{m}$ ($p=0.021$ compared with CCl_4 rats). Post hoc analysis by Fisher's LSD test indicated that T-EVs did not improve microglia activation ($262 \pm 46 \mu\text{m}$, $p=0.035$ compared with controls) (Fig. 6A). None of the EVs affect microglia in control rats.

Rats with mild liver damage also show activation of astrocytes in hippocampus, measured as increase in GFAP staining in hippocampus of 4–7 rats per group. Data were analysed by One-way ANOVA (C-EVs: $F(3, 18)=2,925$, $p=0.062$ and T-EVs: $F(3, 17)=3,060$, $p=0.057$). Post hoc analysis by Fisher's LSD test indicated that the area stained by GFAP increased to $113 \pm 5\%$ of controls ($p=0.04$) in CCl_4 rats. T-EVs treatment improves astrocytes activation in CCl_4 rats, reducing the area stained by GFAP to $104 \pm 7\%$, although difference with CCl_4 rats not reach significance ($p=0.32$). C-EVs did not improve astrocytes activation ($114 \pm 4\%$ of controls, $p=0.019$). Both types

of EVs induce astrocytes activation in control rats ($112 \pm 3\%$ of controls in control rats treated with C-EVs ($p=0.053$) and $121 \pm 7\%$ in rats treated with T-EVs ($p=0.011$) (Fig. 6B).

The content of IL-1β was analyzed by immunohistochemistry in glia and in neurons of the CA1 layer. IL-1β staining was analysed in whole hippocampus parenchyma from 3 to 7 rats per group. Data were analysed by One-Way ANOVA ($F(3, 23)=4,207$, $p=0.016$ for C-EVs and $F(3, 17)=5,895$, $p=0.006$ for T-EVs). Post hoc analysis with Fisher's LSD test showed that rats with mild liver damage show increased content of IL-1β in glia ($189 \pm 17\%$ of control rats, $p=0.0087$) and C-EVs treatment tended to normalize IL-1β content in glia, but the reduction did not reach statistical significance ($148 \pm 16\%$, $p=0.15$). In the case of T-EVs treatment, the analysis with Tukey's multiple comparisons test showed complete normalization of IL-1β staining in CCl_4 rats treated with T-EVs ($112 \pm 7\%$, $p=0.034$ compared with CCl_4 rats without treatment) (Fig. 6C).

IL-1β mean intensity in CA1 was calculated in 5–8 rats per group (5 images per animal). One-way ANOVA ($F(3, 22)=4,019$, $p=0.02$ for C-EVs and $F(3, 25)=6,549$, $p=0.002$, for T-EVs) was followed by Fisher's LSD test for C-EVs. Rats with mild liver damage show reduced content of IL-1β in CA1 neurons (23.6 ± 0.5 arbitrary units (a.u.) compared with 27.7 ± 0.84 a.u. in control rats, $p=0.0025$) which was normalized by C-EVs (26.6 ± 1.2 a.u., $p=0.025$ compared with CCl_4 rats without treatment). Tukey's multiple comparisons test showed that T-EVs treatment had no effect on the content of IL-1β in CA1 neurons from CCl_4 rats (24 ± 1 a.u., $p=0.019$ compared with controls) (Fig. 6D).

The total content of IL-1β in hippocampal homogenates was also analyzed by Western blot. Statistical analysis of data from 9–10 rats per group with One-way ANOVA followed by the Fisher's LSD test indicated no significant differences between groups ($F(5, 53)=0,4297$, $p=0.83$). This result suggests that the changes in glia compensate those in neurons (Fig. 6E). Content of TNF-α in the hippocampus was measured by western blot in 7–10 rats per group. One-way ANOVA ($F(3, 34)=4,660$, $p=0.0078$ for C-EVs and $F(3, 32)=4,983$, $p=0.006$ for T-EVs) was followed by Fisher's LSD test. The total content of TNFα in hippocampus was increased in rats with mild liver damage ($153 \pm 15\%$ of control rats, $p=0.013$). This increase was reversed by C-EVs ($86 \pm 14\%$, $p=0.003$ compared with CCl_4 rats without treatment) but not by T-EVs ($157 \pm 17\%$ of controls, $p=0.040$ compared with controls) (Fig. 4F). Treatment with T-EVs increased the total content of TNFα in hippocampus of control rats ($209 \pm 34\%$ of controls, $p=0.006$) (Fig. 6F).

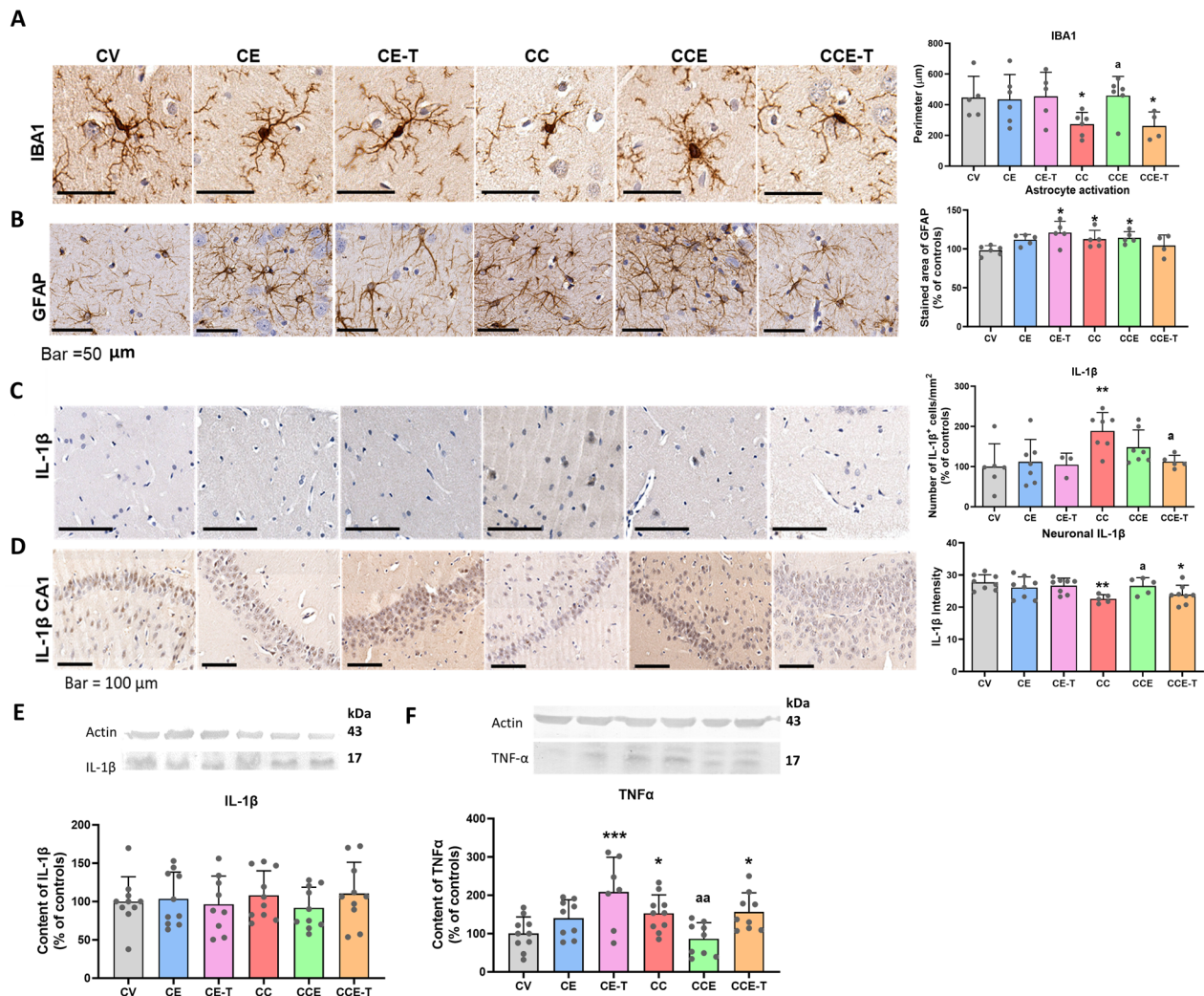


Fig. 6 Effects of MSC-EVs on microglial and astrocytic activation in the hippocampus. **A** Representative images of microglia stained with anti-IBA-1 and its quantification as mean ± SD of 4–6 rats per group. Data were analysed by Kruskal–Wallis test followed by the Uncorrected Dunn’s test for C-EVs (Statistic = 7,496, $p = 0.058$) and by One-way ANOVA followed by Fisher’s LSD test for T-EVs ($F(3, 16) = 3853$, $p = 0.030$). **B** Representative images of astrocytes stained with anti-GFAP and quantification as mean ± SD of 4–7 rats per group. Data were analysed by One-way ANOVA followed by Fisher’s LSD test: C-EVs $F(3, 18) = 2,925$, $p = 0.062$ and T-EVs $F(3, 17) = 3,060$, $p = 0.057$. **C** Representative images of IL-1β immunostaining in hippocampus. Number of IL-1β+ cells is expressed as percentage of control rats and represented as mean ± SD of 3–7 rats per group. Data were analysed by One-Way ANOVA followed by Fisher’s LSD test for C-EVs ($F(3, 23) = 4,207$, $p = 0.016$) and followed by Tukey’s multiple comparisons test for T-EVs ($F(3, 17) = 5,895$, $p = 0.006$). **D** Representative images of IL-1β staining in CA1 region. Values of IL-1β mean intensity in CA1 are represented as mean ± SD of 5–8 rats per group (5 images per animal). One-way ANOVA was followed by Fisher’s LSD test for C-EVs ($F(3, 22) = 4019$, $p = 0.02$) and by Tukey’s multiple comparisons test for T-EVs ($F(3, 25) = 6549$, $p = 0.002$). **E** Content of IL-1β in the hippocampus, measured by western blot, is expressed as mean ± SD of 9–10 rats per group. Data were analysed with One-way ANOVA followed by the Fisher’s LSD test: $F(5, 53) = 0.4297$, $p = 0.83$. **F** Content of TNF-α in the hippocampus, measured by western blot, is expressed as mean ± SD of 7–10 rats per group. One-way ANOVA (C-EVs $F(3, 34) = 4660$, $p = 0.0078$; T-EVs $F(3, 32) = 4,983$, $p = 0.006$) was followed by Fisher’s LSD test. Asterisks indicate a significant difference compared with CV group * $p < 0.05$, *** $p < 0.001$, and “a” compared with CC group $p < 0.05$, aa $p < 0.01$. Full-length blots are presented in the Supplementary Figs. 5E and F

Discussion

The results reported are summarized in Fig. 7. Rats with mild liver damage show impaired hippocampal-dependent spatial learning and memory, as previously shown [5] and treatment with EVs from MSC reverse cognitive

impairment. Impairment of spatial learning and memory is due to altered neurotransmission in the hippocampus which in turn is mainly induced by neuroinflammation in rats with mild liver damage and MHE [5]. Beneficial effects of MSC-EVs from different origins have been

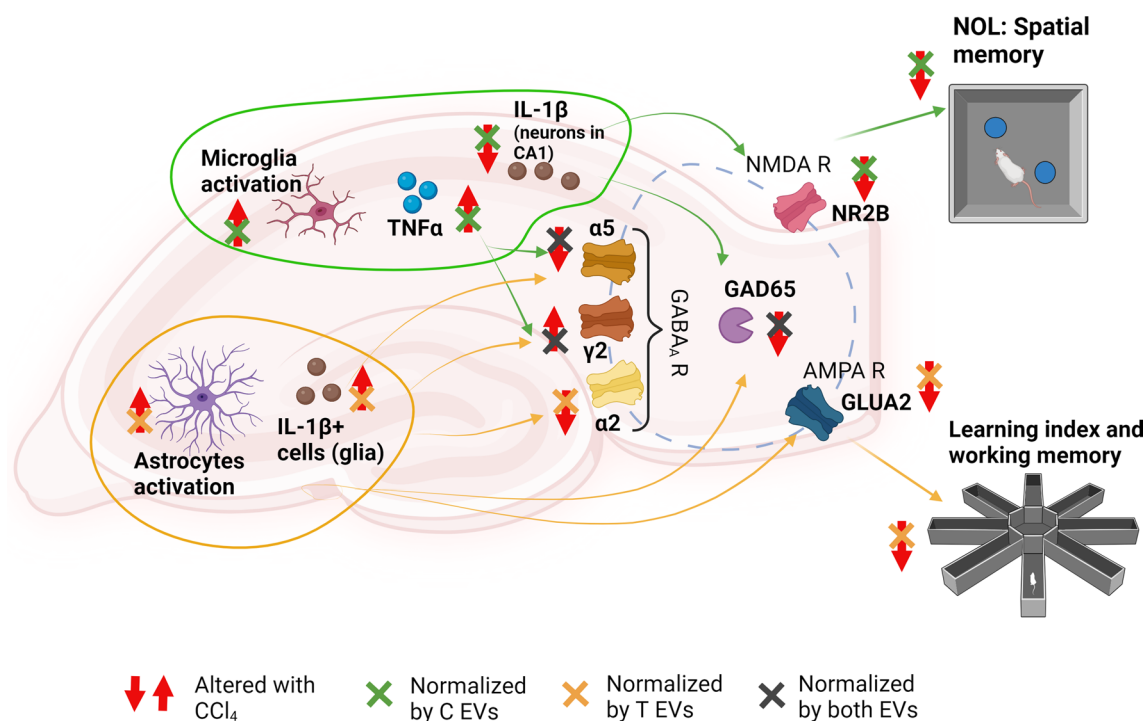


Fig. 7 Proposed scheme summarizing the effects induced by mild liver damage and by MSC-EVs on neuroinflammation, neurotransmission and cognitive function. Mild liver damage induces neuroinflammation, with microglia activation, increase of TNF- α and decrease of IL-1 β in CA1 neurons, which would alter membrane expression of NR2B subunit of NMDA receptors and of the $\alpha 5$ and $\gamma 2$ subunits of the GABA $_A$ receptor, leading to impaired memory in the novel object location (NOL). This mechanism is reversed by C-EVs. Mild liver damage also induces astrocytes activation and increased IL-1 β in glial cells which would decrease membrane expression of GluA2 subunit of the AMPA receptor and of the $\alpha 2$ and $\gamma 2$ subunits of the GABA $_A$ receptor, leading to reduced learning index and working memory. This mechanism is reversed by T-EVs. Created with Biorender.com

reported in several neurological and neurodegenerative pathologies, associated to neuroprotection and reduction of neuroinflammation [33, 34].

The presence of systemically administered EVs into the brain has been previously reported in other studies. Dar et al. [35] also showed the presence of systemically administered EVs in the brain in vivo, by using a fluorescent labelling different from that used in the present work. These authors also demonstrated that a siRNA present in these EVs was released into the brain and induced specific effect in different brain regions, thus supporting an effective transport of EVs into the brain. Chen et al. [36] and Cui et al. [37] also reported evidences for the presence of peripherally administered MSC-EVs into the brain. Although some strategies have been developed to improve the entry of EVs through the blood–brain barrier (BBB) by avoiding their phagocytosis by macrophages and processing in the liver, it has been shown that even without any modification EVs cross the BBB in a good proportion [38]. The presence of EVs after systemic administration is greater in the liver than in the brain. It is possible that improvement of liver damage and/or peripheral inflammation could

contribute to the beneficial effects of MSC-EVs. However, we have previously shown that MSC-EVs reach different brain regions, co-localizing with neurons and microglia cells. Moreover, addition of MSC-EVs ex-vivo to hippocampal slices induce direct beneficial effects on neuroinflammation and neurotransmission, supporting a direct beneficial effect of MSC-EVs into the brain [11].

Modulation of neurotransmission in the hippocampus by systemic administration of MSC-EVs has not been investigated. Deng et al. [39] reported an improvement of hippocampal excitatory synaptic transmission and LTP by EVs derived from bone marrow MSCs in ischemia, leading to improvement of spatial learning and memory. Bone marrow MSC-EVs prevent glutamate excitotoxicity by increasing the glutamate transporter GLT-1 in traumatic brain injury [40]. In rats with hyperammonemia and MHE, altered membrane expression of glutamate receptor subunits is reversed in ex-vivo hippocampal slices by treatment with C-EVs, but not by T-EVs, [11].

The effects of MSC-EVs on spatial learning and memory depends on the type of task and also on the type of EVs (Table 1).

Table 1 Main alterations found in the behaviour, neurotransmission and neuroinflammation in CCl₄ rats and effects of C-EVs and T-EVs on these alterations

	ALTERATION	CCl ₄	Improved by C-EVs	Improved by T-EVs
Behavior	Learning index and working memory	↓		↑
	NOL	↓	↑	
Neurotransmission	NR2B (NMDA)	↓	↑	
	GluA2 (AMPA)	↓		↑
	GAD65	↓	↑	↑
	GAD67	↓		
	GABA _A -α2	↑		↓
	GABA _A -α5	↓	↑	↑
	GABA _A -γ2	↑	↓	↓
	GABA _A -β3	↓		
	NKCC1	↑		↓
	Neuroinflammation	Microglia activation	↑	↓
Astrocytes activation		↑		↓
IL-1β in CA1		↓	↑	
IL-1β ⁺ cells		↑		↓
TNF-α		↑	↓	

Red arrows indicate alterations produced by CCl₄, green arrows indicate normalization by C-EVs, orange arrows indicate normalization by T-EVs

Unmodified MSCs-EVs improve object location memory but not spatial learning or working memory. This is associated with reversal of some but not all the changes in neurotransmission. C-EVs reverse the changes in membrane expression of the NR2B subunit of NMDA receptors and of the γ2 and α5 subunits of GABA_A receptors. C-EVs also reverse some neuroinflammation parameters: microglia activation, the increase in TNF-α and the decrease of IL-1β in CA1 neurons.

Performance in the novel object location (NOL) task has been related with GABAergic neurotransmission. Decreased GABA_A-α5 [41] or GABA_A-β3 subunits [42], as well as decreased expression of NR2B in the hippocampus [43] impairs NOL performance.

It seems therefore that reduced membrane expression of α5 and β3 subunits of GABA_A receptors and of the NR2B subunit of NMDA receptors in the hippocampus of CCl₄ treated rats would contribute to impairment of

NOL. C-EVs do no reverse changes in the β3 subunit and only partially those in the α5 subunit, but reverses completely the reduction in membrane expression of NR2B. The reversal of the changes in α5 and NR2B subunits would be involved in the improvement of NOL memory in CCl₄ rats by C-EVs.

Regarding the role of neuroinflammation, C-EVs reverse microglia activation, the increase in TNF-α levels and the reduction of IL-1β in CA1 neurons in the hippocampus. Elevated TNF-α levels in the hippocampus have been also associated to impaired NOL test [42]. Then, the decrease of TNF-α induced by C-EVs would also contribute to improvement of spatial memory in this NOL task.

A decrease of IL-1β has been reported in other situations associated with neuroinflammation. For example, [44] reported a decrease in IL-1β in parallel with increased IL-6 levels in the hippocampus after alcohol administration, which was associated with impairment of recognition memory.

IL-1β modulates GABA and glutamate receptors subunits expression and function. Increased IL-1β induces an increase in NR2B receptor [45] and in GABA_A-α5 subunit membrane expression and function [46]. Increased IL-1β in CA1 increases GABA receptor currents [47]. In the hippocampus of hyperammonemic rats increased IL-1β content increases membrane expression of NR2B and blocking the IL-1 receptor reverses this increase [48] It is therefore likely that the reduction of membrane expression of the GABA_A-α5 and NR2B subunits in hippocampus of CCl₄ rats would be associated with the reduced levels of IL-1β in CA1 neurons. C-EVs would reverse the reduction in α5 and NR2B membrane expression by normalizing the IL-1β levels in CA1 neurons. This, in turn would improve performance in the NOL test as discussed above.

The beneficial effects of C-EVs would be due to the mechanism summarized in Fig. 7. C-EVs reverse activation of microglia, the increase in TNFα and the reduction of IL-1β in CA1 neurons. This reduction in IL-1β in CA1 neurons would be responsible for the reduced membrane expression of the α5 subunit of GABA receptors and of the NR2B subunit of NMDA receptors which, in turn, would contribute to the impairment of performance in the NOL test. C-EVs reverses the reduction of IL-1β in CA1 neurons and in membrane expression of the α5 and NR2B subunits, reversing therefore the impairment in NOL.

These beneficial effects of C-EVs are completely lost in T-EVs, derived from TGFβ-depleted MSCs.

In contrast, the mechanism of action and the beneficial effects of T-EVs are completely different from those of C-EVs (Fig. 7). T-EVs reduce astrocytes activation

and the increase in the number of IL-1 β ⁺ (glial) cells in the hippocampus (not in CA1 neurons) and, in addition to GABA_A- α 5 and γ 2 subunits, T-EVs also reverse the increase in membrane expression of the GABA_A- α 2 subunit and of NKCC1, and the reduced membrane expression of the glutamate receptor subunit GluA2. This leads to improvement of the impairment in learning and working memory in the radial maze (Fig. 7).

These data suggest that astrocytic activation can be responsible for the increase in glial IL-1 β , which would induce the increase in membrane expression of the GABA_A- α 2 subunit and the decrease in GluA2 membrane expression, which in turn, would induce the impairment in learning and working memory in the radial maze (Fig. 7). These steps in the sequence of events shown in Fig. 7 are normalized by T-EVs treatment but not by C-EVs, suggesting that silencing TGF β facilitates reversal of these changes and improvement of learning and working memory, in contrast to unmodified EVs. As shown in Fig. 1B, silencing TGF β in MSCs results in changes in the content of 14 proteins in the EVs (T-EVs) as analysed by proteomics and a mild reduction of the precursor of TGF β as analysed by Western blot. It is possible that changes in proteins other than TGF β could contribute to the differential effects of T-EVs and C-EVs. A role for TGF β in the EVs in the modulation of neuroinflammation and alterations in neurotransmission has been previously shown by Izquierdo-Altarejos et al. [11]. They showed that ex vivo treatment of hippocampal slices from hyperammonemic rats with EVs from MSCs reverses microglial and astrocytic activation and normalizes TNF α and IL-1 β content and induces a shift from a pro-inflammatory to an anti-inflammatory state. The capacity of EVs from MSCs to reverse microglia and astrocytes activation ex vivo was eliminated when the EVs were co-incubated with anti-TGF β or when EVs from TGF β -silenced MSCs were used, thus supporting that TGF β in the surface of the EVs is inducing these effects. Izquierdo-Altarejos et al. [11] also showed that ex vivo treatment with MSC-EVs reverses the alterations in membrane expression of AMPA and NMDA receptors in hippocampal slices from hyperammonemic rats. This normalization did not occur in the presence of anti-TGF β or when EVs from TGF β -silenced MSCs were used. They propose that TGF β in the surface of MSCs EVs is a main contributor to the normalization of membrane expression of NMDA and AMPA receptor subunits in hyperammonemic rats. This suggests that TGF β per se would be a main contributor to the beneficial effects of C-EVs. The results reported here suggest that, in addition to TGF β , other proteins present in the EVs,

especially in the T-EVs also induce beneficial effects by different mechanisms.

Previous studies support the participation of the mentioned above astrocytes- IL-1 β —GluA2 pathway in the impairment of working memory. Astrocytes participate in the modulation of working memory [49, 50]. Astrocytes activation in the hippocampus has been associated with impairment of spatial learning and working memory in the radial maze, induced by methamphetamine [51]. Increased hippocampal IL-1 β contributes to memory impairment in rats with peripheral inflammation or chronic hyperammonemia [25], [52]. Also, a decrease in synaptic GluA2 has been related to impairment of spatial learning and memory in rats subjected to acute stress or treated with metamphetamine [51, 53]. Also, reduced GluA2 membrane expression is associated to spatial memory impairment in the radial maze in hyperammonemic rats [7]. Increased membrane expression of the Cl⁻ co-transporter NKCC1 in the hippocampus has been also associated with repeated stress and cognitive and social behaviour alterations [54]. Then, reversion of the increase of NKCC1 membrane expression by T-EVs in rats with mild liver damage can also contribute to the improvement of cognitive function by treatment with these EVs.

These results highlight the important role played by EVs in modulating neuroinflammation, neurotransmission and cognitive function. Moreover, they highlight the versatility of EVs in modulating these processes, mild changes in the cargo of the EVs (in this case the depletion of TGF β) induce strong changes in the effects of the EVs and in the mechanisms involved. We summarize these changes and effects in Table 1.

Although we have not found beneficial effects of systemic administration of MSCs-EVs on the parameters analysed of liver damage at the histological level or on release of hepatic enzymes to blood, we cannot rule out that MSC-EVs could induce beneficial effects on other aspects of liver damage. In fact, several reports show beneficial effect of MSC-EVs on CCl₄-induced liver injury. For example, Qu et al. [55] show that exosomes derived from MSCs overexpressing miR-181-5p, but not those injected with control MSC-derived EVs, prevent liver fibrosis after 8 weeks of CCl₄ administration. Other studies also show beneficial effects of MSC-EVs on fibrotic liver in mice and rats injected with CCl₄ for six-eight weeks [56–58]. Discrepancies with our present work could be explained by small differences in CCl₄ dose or weeks of administration. To clarify this discrepancy, a more detailed analysis of the effects of both types of EVs on other parameters reflecting other aspects of liver damage will be performed in the next future.

Conclusions

This work shows that treatment with MSC-EVs improves learning and memory in a model of mild liver damage and MHE in rats, suggesting that MSC-EVs may be a good therapeutic option to reverse cognitive impairment in patients with steatotic liver disease.

It is shown that EVs from normal MSCs (C-EVs) improve some aspects of neuroinflammation (microglia activation and TNF α and IL-1 β levels in CA1 neurons) and of neurotransmission (α 5 and γ 2 subunits of GABA $_A$ receptors and NR2B subunit of NMDA receptors) and improve object location memory. These beneficial effects are lost in EVs from TGF β -depleted MSCs (T-EVs), suggesting a role of TGF β in the beneficial effects. T-EVs improve other aspects of neuroinflammation (astrocytes activation, IL-1 β levels in glial cells) and of neurotransmission (α 2 and γ 2 subunits of GABA $_A$ receptors and GluA2 subunit of AMPA receptors) and improve working memory impairment.

All the beneficial effects induced by C-EVs are not induced by T-EVs and the beneficial effects of T-EVs are not induced by C-EVs. This suggests that TGF β plays a key role in triggering the beneficial effects of C-EVs. This also indicates that depletion of TGF β in MSCs induces changes in the cargo of the EVs that allow triggering effects which are not induced by normal EVs. The mechanisms by which these effects are induced remain unclear. It is possible that depletion of TGF β in MSCs may lead to changes in the expression of other proteins which could trigger the beneficial effects induced by T-EVs. Another possibility is that these mechanisms are triggered by proteins already present in C-EVs but are prevented by the presence of TGF β . Further studies to unveil the mechanisms by which T-EVs induce their beneficial effects could help to design new modifications of MSCs directed to produce EVs able to induce simultaneously the beneficial effects of C-EVs and T-EVs. This would enhance the therapeutic potential of these EVs.

Abbreviations

CCl ₄	Carbon tetrachloride
DAB	Diaminobenzidine
EV	Extracellular vesicles
C-EVs	Wild type EV
T-EVs	EV from TGF β knockdown MSCs GABA: γ -aminobutyric acid
GAD	Glutamate decarboxylase
GAT	GABA transporter
GFAP	Glial fibrillary acidic protein
GluA	AMPA glutamate receptor subunit
IBA1	Ionized calcium binding adaptor molecule 1
KCC2	Potassium chloride cotransporter 2
MHE	Minimal hepatic encephalopathy
MLD	Mild liver damage
MSC	Mesenchymal stem cells
NKCC1	Na–K–Cl cotransporter 1
NOL	Novel object location
NR	NMDA glutamate receptor subunit
SLD	Steatotic liver disease

TGF β	Transforming growth factor β
TNF α	Tumor necrosis factor α

Supplementary Information

The online version contains supplementary material available at <https://doi.org/10.1186/s13287-024-04076-6>.

Additional file 1
Additional file 2
Additional file 3
Additional file 4
Additional file 5
Additional file 6
Additional file 7
Additional file 8
Additional file 9
Additional file 10
Additional file 11
Additional file 12
Additional file 13
Additional file 14
Additional file 15
Additional file 16
Additional file 17
Additional file 18
Additional file 19
Additional file 20

Acknowledgements

The authors declare that they have not used Artificial Intelligence in this study.

Author contributions

MG: investigation, formal analysis, validation, writing of the original draft, visualization; VM-M: resources, supervision, visualization, writing of the original draft; VF: conceptualization, funding acquisition, project administration, supervision, visualization, writing (review and editing); ML: formal analysis, funding acquisition, supervision, validation, visualization, writing of the original draft, review and editing.

Funding

This work was supported in part by Ministerio de Ciencia e Innovación Spain (PID2020-113388RB-I00; MICIU/AEI/<https://doi.org/10.13039/501100011033>); Conselleria Educació, Universidades y Ocupació, Generalitat Valenciana (CIPROM 2021/082); European Regional Development Funds / ERDF (PID2020-113388RB-I00 and CIPROM 2021/082); Part of the equipment employed in this work has been funded by Generalitat Valenciana and co-financed with ERDF funds (OP ERDF of Comunitat Valenciana 2014–2020). GM has an FPU contract (FPU18/03851) from Ministerio de Ciencia e Innovación Spain.

Availability of data and materials

The data that support the findings of this study are available from the corresponding author upon reasonable request. Data of EV proteomic analysis are included as Supplementary files: Proteomic analysis 1–30 (RESULTS VF MLI EVs DIANN).

Declarations

Ethics approval and consent to participate

The experiments were approved by the Ethic Committee (Comité Ético de Experimentación Animal, CEEA) of Centro de Investigación Príncipe Felipe (Tratamiento con exosomas de células mesenquimales en modelos animales de encefalopatía hepática. Mecanismos implicados, no 2019-21, approved on 02-06-2020) and the Conselleria de Agricultura de la Generalitat Valenciana (2020/VSC/PEA/0042, approved on 03-03-2020) and they were performed in accordance with the guidelines of the Directive of the European Commission (2010/63/EU) for the care and handling of experimental animals. The work has been reported in line with the ARRIVE guidelines 2.0. All donors of subcutaneous fat gave written informed consent, and all procedures complied with the principles of the Declaration of Helsinki and were approved by the Ethics Committee of the Basque Country Health System (CEIC-E, Spain; Protocol no. E08-30).

Consent for publication

Not applicable.

Competing interests

The authors declare that they have no competing interests.

Author details

¹Laboratory of Neurobiology, Centro de Investigación Príncipe Felipe, Eduardo Primo Yúfera, 3, 46012 Valencia, Spain. ²Neuronal and Tissue Regeneration Laboratory, Centro Investigación Príncipe Felipe, Valencia, Spain.

Received: 19 June 2024 Accepted: 22 November 2024

Published online: 18 December 2024

References

- Felipo V. Hepatic encephalopathy: effects of liver failure on brain function. *Nat Rev Neurosci*. 2013;14(12):851–8.
- Hüssinger D, Görg B, Gomez MR, Schnitzler A, Robinson SDT. Hepatic encephalopathy. *Nat Rev Dis Prim*. 2022;8(1):43.
- Giménez-Garzó C, Fiorillo A, Ballester-Ferré MP, Gallego JJ, Casanova-Ferrer F, Urios A, Benlloch S, Martí-Aguado D, San-Miguel T, Tosca J, Ríos MP, Montón C, Durbán L, Escudero-García D, Aparicio L, Felipo V, Montoliu C. A new score unveils a high prevalence of mild cognitive impairment in patients with nonalcoholic fatty liver disease. *J Clin Med*. 2021;10(13):1–18.
- Leone P, Arenas YM, Balzano T, Mincheva G, Garcia MM, Montoliu C, Llansola M, Felipo V, Felipe IP. Patients who died with steatohepatitis or liver cirrhosis show neuroinflammation and neuronal loss in hippocampus. *Eur J Neurol*. 2023. <https://doi.org/10.1111/ene.15935>.
- Leone P, Mincheva G, Balzano T, Malaguarnera M, Felipo V, Llansola M. Rifaximin improves spatial learning and memory impairment in rats with liver damage-associated neuroinflammation. *Biomedicines*. 2022;30(10):3032–46.
- Hernández-Rabaza V, Cabrera-Pastor A, Taoro-González L, Malaguarnera M, Agustí A, Llansola M, Felipo V. Hyperammonemia induces glial activation, neuroinflammation and alters neurotransmitter receptors in hippocampus, impairing spatial learning: Reversal by sulforaphane. *J Neuroinflammation*. 2016. <https://doi.org/10.1186/s12974-016-0505-y>.
- Cabrera-Pastor A, Hernandez-Rabaza V, Taoro-Gonzalez L, Balzano T, Llansola M, Felipo V. In vivo administration of extracellular cGMP normalizes TNF- α and membrane expression of AMPA receptors in hippocampus and spatial reference memory but not IL-1 β , NMDA receptors in membrane and working memory in hyperammonemic rats. *Brain Behav Immun*. 2016;57:360–70.
- Balzano T, Dadsetan S, Forteza J, Cabrera-Pastor A, Taoro-Gonzalez L, Malaguarnera M, Gil-Perotin S, Cubas-Nuñez L, Casanova B, Castro-Quintas A, Ponce-Mora A, Arenas YM, Leone P, Erceg S, Llansola M, Felipo V. Chronic hyperammonemia induces peripheral inflammation that leads to cognitive impairment in rats: reversed by anti-TNF- α treatment. *J Hepatol*. 2020;73(3):582–92.
- Sánchez-Castillo VE, Sepúlveda AI, Marín-Teva MR, Cuadros JL, Martín-Oliva MA, González-Rey D, Delgado E, Neubrand M. Switching roles : beneficial effects of adipose tissue-derived mesenchymal stem cells on microglia and their implication in neurodegenerative diseases. *Biomolecules*. 2022;12:219.
- Harrell CR, Volarevic V, Djonov V. Therapeutic potential of exosomes derived from adipose tissue-sourced mesenchymal stem cells in the treatment of neural and retinal diseases. *Int J Mol Sci*. 2022;23:4487.
- Altarejos PI, Pastor AC, García MM, Huertas CS, Hernández A, Manzano VM, Felipo V. Extracellular vesicles from mesenchymal stem cells reduce neuroinflammation in hippocampus and restore cognitive function in hyperammonemic rats. *J Neuroinflammation*. 2023;20:1–28.
- Huang Z, Xu A. Adipose extracellular vesicles in intercellular and inter-organ crosstalk in metabolic health and diseases. *Front Immunol*. 2021;12:608680.
- Massagué J, Sheppard D. TGF- β Signaling in Health and Disease. *Cell*. 2023;186(19):4007–37.
- Wells RG. V. TGF- β signaling pathways. *Am J Physiol Gastrointest Liver Physiol*. 2000;279:845–50.
- Worthington JJ, Fenton TM, Czajkowska BJ, Klementowicz JE, Travis MA. Immunobiology Regulation of TGF- β in the immune system : An emerging role for integrins and dendritic cells. *Immunobiology*. 2012;217(12):1259–65.
- Banchereau J, Pascual V, O'Garra A. From IL-2 to IL-37: the expanding spectrum of anti-inflammatory cytokines. *Nat Immunol*. 2012;13(10):925–31.
- Vitkovic L, Maeda S, Sternberg E. Anti-inflammatory cytokines : expression and action in the brain. *Neuroimmunomodulation*. 2001;9:295–312.
- Basu A, Krady JK, Enterline JR, Levison S. Transforming growth factor β 1 prevents IL-1 α -induced microglial activation, whereas TNF α - and IL-6-stimulated activation are not antagonized. *Glia*. 2002;40:109–20.
- Chen J, Ke K, Lu J, Qiu Y, Peng Y. Protection of TGF- β 1 against neuroinflammation and neurodegeneration in A β 1–42 -induced Alzheimer 's disease model rats. *PlosOne*. 2015;10(2):e0116549.
- Lee GP, Il Jeong W, Jeong DH, Do SH, Kim TH, Jeong KS. Diagnostic evaluation of carbon tetrachloride-induced rat hepatic cirrhosis model. *Anticancer Res*. 2005;25:1029–38.
- Balzano T, Leone P, Ivaylova G, Carmen Castro M, Reyes L, Ramón C, Malaguarnera M, Llansola M, Felipo V. Rifaximin prevents T-lymphocytes and macrophages infiltration in cerebellum and restores motor incoordination in rats with mild liver damage. *Biomedicines*. 2021. <https://doi.org/10.3390/biomedicines9081002>.
- Castro B, Martínez-Redondo D, Gartzia I, Alonso-Varona A, Garrido P, Palomares T. Cryopreserved H₂O₂ preconditioned human adipose - derived stem cells exhibit fast post: thaw recovery and enhanced bioactivity against oxidative stress. *J Tissue Eng Regen Med*. 2019;13:328–41. <https://doi.org/10.1002/term.2797>.
- Meier F, Brunner AD, Frank M, Ha A, Bludau I, Voytik E, Kaspar-Schoenefeld S, Lubeck N, Raether O, Bache N, Aebbersold R, Collins BC, Röst HL, Man M, et al. diaPASEF: parallel accumulation–serial fragmentation combined with data-independent acquisition. *Nat Methods*. 2020;17:1229–36. <https://doi.org/10.1038/s41592-020-00998-0>.
- Kleiner DE, Brunt EM, Van Natta M, Behling C, Contos MJ, Cummings OW, Ferrell LD, Liu YC, Torbenson MS, Unalp-Arida A, Yeh M, McCullough AJ, Sanyal AJ. Design and validation of a histological scoring system for non-alcoholic fatty liver disease: nonalcoholic steatohepatitis clinical research network. *Hepatology*. 2005;41(6):1313–21. <https://doi.org/10.1002/hep.20701>.
- Taoro-González L, Cabrera-Pastor A, Sancho-Alonso M, Arenas YM, Meseguer-Estornell F, Balzano T, Elmili N, Felipo V. Differential role of interleukin-1 β in neuroinflammation-induced impairment of spatial and nonspatial memory in hyperammonemic rats. *FASEB J*. 2019;33(9):9913–28.
- Felipo V, Miñana MD, Grisolia S. Long-term ingestion of ammonium increases acetylglutamate and urea levels without affecting the amount of carbamoyl-phosphate synthase. *Eur J Biochem*. 1988;176(3):567–71.
- Cabrera-Pastor A, Taoro L, Llansola M, Felipo V. Roles of the NMDA receptor and EAAC1 transporter in the modulation of extracellular glutamate by low and high affinity AMPA receptors in the cerebellum in vivo: differential alteration in chronic hyperammonemia. *ACS Chem Neurosci*. 2015;6(12):1913–21.

28. Möhler H, Rudolph U, Boison D, Singer P, Feldon J, Yee BK. Pharmacology, biochemistry and behavior regulation of cognition and symptoms of psychosis: focus on gaba receptors and glycine transporter 1. *Pharmacol Biochem Behav.* 2008;90:58–64.
29. Johansson M, Agusti A, Llansola M, Montoliu C, Strömberg J, Malinina E, Ragagnin G, Doverskog M, Bäckström T, Felipe V. GR3027 antagonizes GABAA receptor-potentiating neurosteroids and restores spatial learning and motor coordination in rats with chronic hyperammonemia and hepatic encephalopathy. *Am J Physiol Gastrointest Liver Physiol.* 2015. <https://doi.org/10.1152/ajpgi.00073.2015>.
30. Malaguarnera M, Llansola M, Balzano T, Gómez-Giménez B, Antúnez-Muñoz C, Martínez-Alarcón N, Mahdini R, Felipe V. Bicuculline reduces neuroinflammation in hippocampus and improves spatial learning and anxiety in hyperammonemic rats. Role of glutamate receptors. *Front Pharmacol.* 2019;10:132.
31. Sakimoto Y, Oo PM, Goshima M, Kanehisa I, Tsukada Y, Mitsushima D. Significance of GABA A receptor for cognitive function and hippocampal pathology. *Int J Mol Sci.* 2021;22:12456.
32. Sancho-alonso M, Arenas YM, Izquierdo-altarejos P, Martínez-garcía M. Enhanced Activation of the S1PR2-IL-1 β -Src-BDNF-TrkB pathway mediates neuroinflammation in the hippocampus and cognitive impairment in hyperammonemic rats. *Int J Mol Sci.* 2023;24:17251.
33. Nakano M, Fujimiya M. Potential effects of mesenchymal stem cell derived extracellular vesicles and exosomal miRNAs in neurological disorders. *Neural Regen Res.* 2021;16(12):2359–66.
34. Skok M. Mesenchymal stem cells as a potential therapeutic tool to cure cognitive impairment caused by neuroinflammation. *World J Stem Cells.* 2021;13(8):1072–84.
35. Dar GH, Mendes CC, Kuan WL, Speciale AA, Conceição M, Görgens A, Uliyakina I, Lobo MJ, Lim WF, El Andaloussi S, Mäger I, Roberts TC, Barker RA, Goberdhan DCI, Wilson C, Wood MJA. GAPDH controls extracellular vesicle biogenesis and enhances the therapeutic potential of EV mediated siRNA delivery to the brain. *Nat Commun.* 2021;12(1):6666. <https://doi.org/10.1038/s41467-021-27056-3>.
36. Chen SY, Lin MC, Tsai JS, He PL, Luo WT, Herschman H, Li HJ. EP(4) antagonist-elicited extracellular vesicles from mesenchymal stem cells rescue cognition/learning deficiencies by restoring brain cellular functions. *Stem Cells Transl Med.* 2019;8(7):707–23. <https://doi.org/10.1002/sctm.18-0284>.
37. Cui GH, Wu J, Mou FF, Xie WH, Wang FB, Wang QL, Fang J, Xu YW, Dong YR, Liu JR, Guo HD. Exosomes derived from hypoxia-preconditioned mesenchymal stromal cells ameliorate cognitive decline by rescuing synaptic dysfunction and regulating inflammatory responses in APP/PS1 mice. *FASEB J.* 2018;32(2):654–68. <https://doi.org/10.1096/fj.201700600R>.
38. Lai N, Wu D, Liang T, Pan P, Yuan G, Li X, Li H, Shen H, Wang Z, Chen G. Systemic exosomal miR-193b-3p delivery attenuates neuroinflammation in early brain injury after subarachnoid hemorrhage in mice. *J Neuroinflammation.* 2020;17(1):74. <https://doi.org/10.1186/s12974-020-01745-0>.
39. Deng M, Xiao H, Zhang H, Peng H, Yuan H, Xu Y, Hermann DM. Mesenchymal stem cell-derived extracellular vesicles ameliorates hippocampal synaptic impairment after transient global ischemia. *Front Cell Neurosci.* 2017;11:205.
40. Zhuang Z, Liu M, Dai Z, Luo J, Zhang B, Yu H, Xue J, Xu H. Bone marrow stromal cells-derived exosomes reduce neurological damage in traumatic brain injury through the miR-124-3p / p38 MAPK / GLT-1 axis. *Exp Neurol.* 2023;365:114408.
41. Prut L, Prenosil G, Willadt S, Vogt K, Fritschy J, Crestani F. A reduction in hippocampal GABA A receptor α 5 subunits disrupts the memory for location of objects in mice. *Genes, Brain Behav.* 2010;9:478–88.
42. Brymer KJ, Fenton EY, Kalyanchuk LE, Caruncho HJ. Peripheral etanercept administration normalizes behavior, hippocampal neurogenesis, and hippocampal reelin and GABA A receptor expression in a preclinical model of depression. *Front Pharmacol.* 2018;9:121.
43. Moraga-amaro R, González H, Ugalde V, Donoso- JP, Quintana-donoso D, Lara M, Morales B, Rojas P, Pacheco R, Stehberg J. Dopamine receptor D5 deficiency results in a selective reduction of hippocampal NMDA receptor subunit NR2B expression and impaired memory. *Neuropharmacology.* 2015;2016:222–35.
44. Terasaki LS, Schwarz JM. brain sciences impact of prenatal and subsequent adult alcohol exposure on pro-inflammatory cytokine expression in brain regions necessary for simple recognition memory. *Brain Sci.* 2017;7:125.
45. Bertani I, Iori V, Trusel M, Maroso M, Foray C, Mantovani XS, Tonini R, Vezani A, Chiesa R. Inhibition of IL-1 signaling normalizes NMDA-dependent neurotransmission and reduces seizure susceptibility in a mouse model of creutzfeldt-jakob disease. *J Neurosci.* 2017;37(43):10278–89.
46. Wang D, Zurek AA, Lecker I, Yu J, Abramian AM, Avramescu S, Davies PA, Moss SJ, Lu W, Orser BA. Report memory deficits induced by inflammation are regulated by a 5-subunit-containing GABA A receptors. *Cell Rep.* 2012;2:488–96.
47. Hellstrom IC, Danik M, Luheshi GN, Williams S. Chronic LPS exposure produces changes in intrinsic membrane properties and a sustained IL- b -dependent increase in GABAergic inhibition in hippocampal CA1 pyramidal neurons. *Hippocampus.* 2005;15:656–64.
48. Taoro-Gonzalez L, Arenas YM, Cabrera-Pastor A, Felipe V. Hyperammonemia alters membrane expression of GluA1 and GluA2 subunits of AMPA receptors in hippocampus by enhancing activation of the IL-1 receptor: Underlying mechanisms. *J Neuroinflammation.* 2018;15(1):1–15.
49. Logan S, Pharaoh GA, Marlin MC, Masser DR, Matsuzaki S, Wronowski B, Yeganeh A, Parks EE, Premkumar P, Farley JA, Owen DB, Humphries KM, Kinter M, Freeman WM, Szweda LI, Van Remmen H, Sonntag WE. Insulin-like growth factor receptor signaling regulates working memory, mitochondrial metabolism, and amyloid- b uptake in astrocytes. *Mol Metab.* 2018;9:141–55.
50. Gordleeva SY, Tsybina YA, Krivososov MI. Modeling working memory in a spiking neuron network accompanied by astrocytes. *Front Cell Neurosci.* 2021;15:631485.
51. Avila JA, Zanca RM, Shor D, Paleologos N, Alliger AA, Figueiredo-pereira ME, Serrano PA. Chronic voluntary oral methamphetamine induces deficits in spatial learning and hippocampal protein kinase Mzeta with enhanced astrogliosis and cyclooxygenase-2 levels. *Heliyon.* 2018. <https://doi.org/10.1016/j.heliyon.2018.e00509>.
52. Barrientos RM, Frank MG, Hein AM, Higgins EA, Watkins LR, Rudy JW, Maier SF. Time course of hippocampal IL-1 beta and memory consolidation impairments in aging rats following peripheral infection. *Brain Behav Immun.* 2009;23(1):46–54.
53. Sebastian V, Estil JB, Chen D, Schrott LM, Serrano PA. Acute Physiological Stress Promotes Clustering of Synaptic Markers and Alters Spine Morphology in the Hippocampus. *PlosOne.* 2013;8(10):e79077.
54. Tsukahara T, Masuhara M, Iwai H, Sonomura T. Biochemical and Biophysical Research Communications Repeated stress-induced expression pattern alterations of the hippocampal chloride transporters KCC2 and NKCC1 associated with behavioral abnormalities in female mice. *Biochem Biophys Res Commun.* 2015;465:145–51.
55. Qu Y, Zhang Q, Cai X, Li F, Ma Z, Xu M, Lu L. Exosomes derived from miR-181-5p-modified adipose-derived mesenchymal stem cells prevent liver fibrosis via autophagy activation. *J Cell Mol Med.* 2017;21(10):2491–502. <https://doi.org/10.1111/jcmm.13170>.
56. Gupta S, Pinky V, Sharma H, Soni N, Rao EP, Dalela M, Yadav A, Nautiyal N, Kumar A, Nayak B, Banerjee A, Dinda AK, Mohanty S. Comparative evaluation of anti-fibrotic effect of tissue specific mesenchymal stem cells derived extracellular vesicles for the amelioration of CCL4 induced chronic liver injury. *Stem Cell Rev Rep.* 2022;18:1097–112. <https://doi.org/10.1007/s12015-021-10313-9>.
57. Gan L, Zheng L, Yao L, Lei L, Huang Y, Zeng Z, Fang N. Exosomes from adipose-derived mesenchymal stem cells improve liver fibrosis by regulating the miR-20a-5p/TGFBR2 axis to affect the p38 MAPK/NF-kappaB pathway. *Cytokine.* 2023;172:156386. <https://doi.org/10.1016/j.cyto.2023.156386>.
58. Yu L, Xue J, Wu Y, Zhou H. Therapeutic effect of exosomes derived from hepatocyte-growth-factor-overexpressing adipose mesenchymal stem cells on liver injury. *Folia Histochem Cytobiol.* 2023;61(3):160–71. <https://doi.org/10.5603/fhc.95291>.

Publisher's Note

Springer Nature remains neutral with regard to jurisdictional claims in published maps and institutional affiliations.